DOI: 10.1002/anie.200704488

Nanotechnology

Carbon Nanotube Gas and Vapor Sensors

*Douglas R. Kauffman and Alexander Star**

Keywords:
carbon nanotubes · field-effect transistors · molecular devices · nanotechnology · sensors

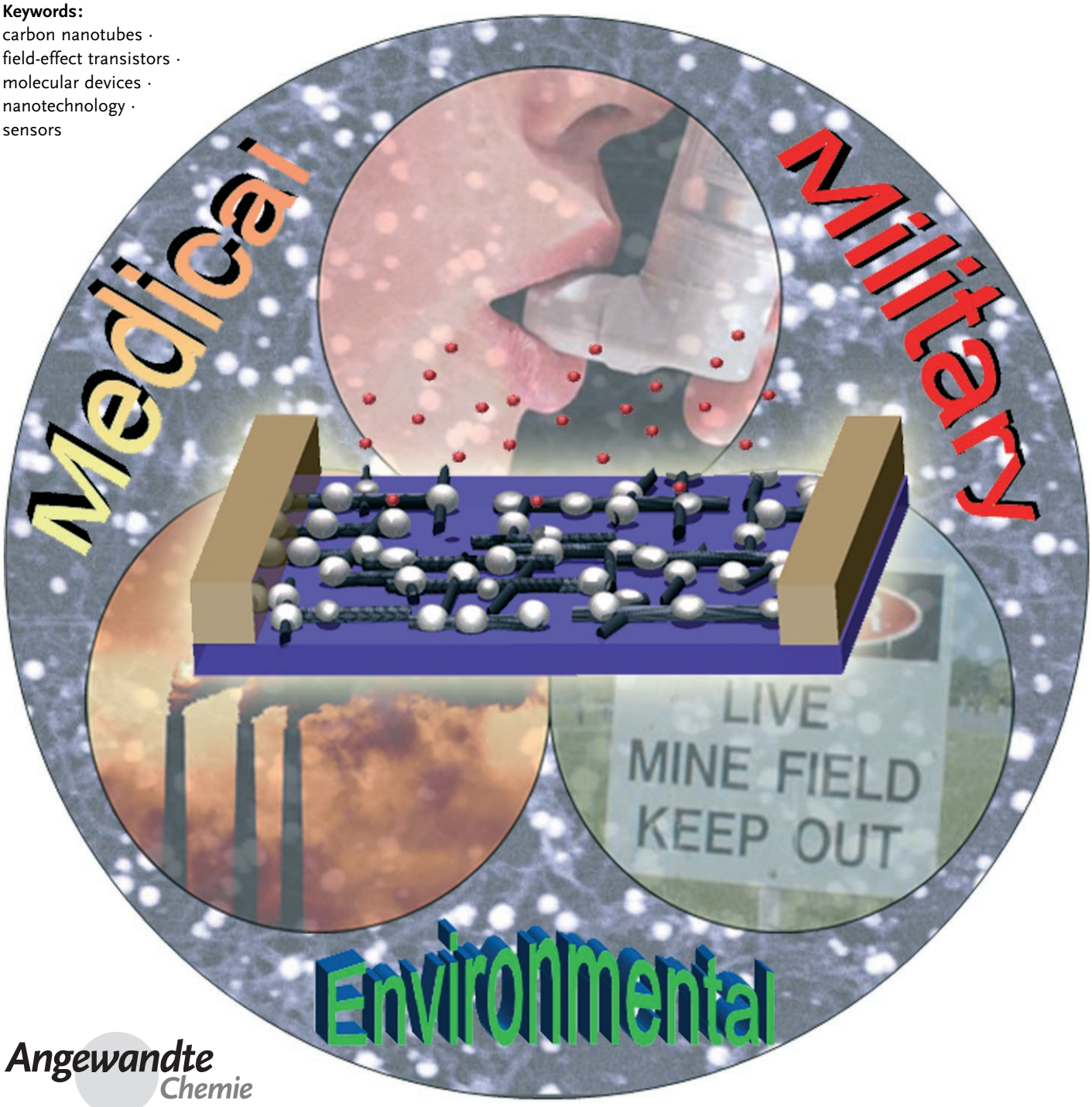

Carbon nanotubes have aroused great interest since their discovery in 1991. Because of the vast potential of these materials, researchers from diverse disciplines have come together to further develop our understanding of the fundamental properties governing their electronic structure and susceptibility towards chemical reaction. Carbon nanotubes show extreme sensitivity towards changes in their local chemical environment that stems from the susceptibility of their electronic structure to interacting molecules. This chemical sensitivity has made them ideal candidates for incorporation into the design of chemical sensors. Towards this end, carbon nanotubes have made impressive strides in sensitivity and chemical selectivity to a diverse array of chemical species. Despite the lengthy list of accomplishments, several key challenges must be addressed before carbon nanotubes are capable of competing with state-of-the-art solid-state sensor materials. The development of carbon nanotube based sensors is still in its infancy, but continued progress may lead to their integration into commercially viable sensors of unrivalled sensitivity and vanishingly small dimensions.

From the Contents

1. Introduction

At the most fundamental level, a chemical sensor can be defined as something that responds to changes in the local chemical environment. For a chemical sensor to be useful, its response must be predictable such that it scales with the magnitude of change in the local chemical environment. Furthermore, a chemical sensor should be sensitive and selective. The development of chemical sensors is a well-established field that has been thoroughly covered in the literature.[1] However, the past several years have witnessed a shift in sensor technology towards more sensitive recognition layers, increasingly complex architectures, and reduced size because of the emergence of nanotechnology. Rapid progress in the synthesis and fundamental understanding of surface phenomena has generated great excitement about incorporation of nanomaterials into sensor architectures.[2] Nanomaterials are strong candidates for analyte detection, because their reduced dimensions create an increase in environmental sensitivity. For example, reducing the dimensions of a material to the order of several nanometers gives surface chemistry events a much more important role than in the bulk state.[3] The reduced dimensionality also creates structures with exceptionally high surface area, and some materials, such as certain types of carbon nanotubes (CNTs), are composed almost entirely of surface atoms. These two consequences of reduced size result in a class of materials that has the potential for unsurpassed sensitivity towards changes in its chemical environment. It has already been speculated that the scaling of silicon-based semiconducting metal oxide technologies will reach its limit in the near future;[4] therefore it is necessary to explore novel materials for sensor design.

From the discovery of carbon nanotubes in 1991[5] until the end of 2007, roughly 30000 scientific reports have been published on this topic. This explosion of CNT reports is illustrated in Figure 1 with a histogram detailing the number of CNT publications per year. This large volume of CNT literature includes over 1200 reports that deal specifically with the application of CNTs in a sensing capacity. The development of CNT-based chemical and biological sensors is a rich field, and these areas have already been the topic of several excellent reviews.[6] We also recently published a review on NTFET-based biosensors (NTFET = nanotube field-effect transistor);[7] therefore this discussion will be limited to CNT-based sensors for gas- and vapor-phase analytes. This

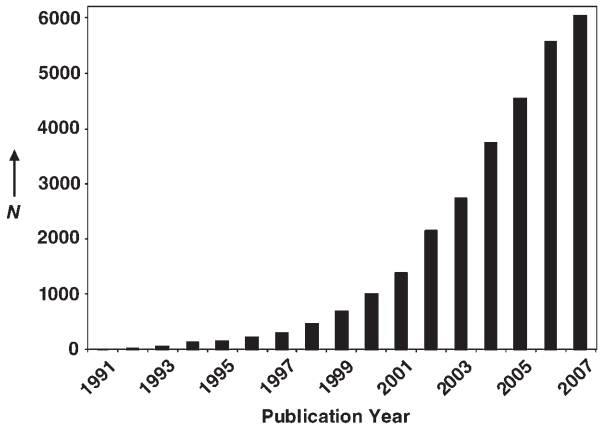

Figure 1. Histogram detailing the number of CNT publications per year between 1991 and 2007 (data obtained from ISI Web of Knowledge).

[*] D. R. Kauffman, Prof. A. Star
Department of Chemistry, University of Pittsburgh and
The National Energy Technology Laboratory, Pittsburgh, PA (USA)
Fax: (+1) 412-624-4027
E-mail: astar@pitt.edu
Homepage: http://www.pitt.edu/~astar

Review is intended to present an overview of the current state of CNT sensor technology, provide a comparison to existing state-of-the-art sensor technology, and present an outlook for the future of CNT-based sensor technologies.

1.1. Properties of Carbon Nanotubes and Carbon Nanotube Devices

Since the discovery of CNTs in 1991 by Iijima,[5] a great deal of effort has been devoted to the application of this new class of materials. A large number of articles has been published on the chemistry and fundamental electronic and physical properties of CNTs,[8,9] so only a brief overview of their electronic structure and integration into electronic devices will be given here.

CNTs are chiral structures that consist of either one single outer wall (single-walled carbon nanotube, SWNT),[10] or multiple concentrically nestled walls (multiwalled carbon nanotube, MWNT; Figure 2A). The construction of a CNT can be conceptualized by rolling a perfect graphene sheet into a cylinder where vectors, termed roll-up vectors (n,m), describe the electronic structure of the CNT.[11] Metallic and semimetallic CNTs have roll-up vectors such that $n-m=3q$ (where q is any integer or zero) and semiconducting CNTs have $n-m\neq 3q$, 0. Figure 2B depicts the orientation of roll-up vectors and the varying types of SWNTs created from different (n,m) values.

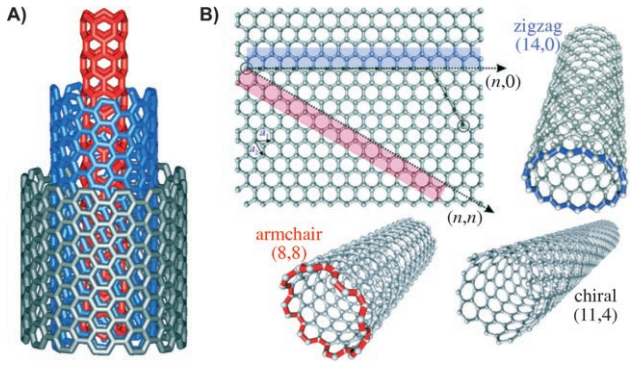

Figure 2. A) Conceptualized depiction of a multiwalled carbon nanotube (MWNT) with concentrically nestled walls. A single-walled carbon nanotube (SWNT) consists of one wall, or the innermost (red) CNT. B) Schematic depiction of the roll-up vectors (n,m) of a CNT, showing armchair ($n=m$), chiral ($n\neq m$), and zigzag (n,0) SWNTs; adapted from reference [11b].

The distinction between semiconducting and metallic CNTs is important in the operation of nanotube-based field-effect transistor (NTFET) devices. The Dekker[12] and Avouris[13] groups first reported the fabrication of NTFETs in 1998. NTFET devices are composed of individual or random networks[14] of CNTs between source (S) and drain (D) electrodes with a Si back gate separated by a SiO_2 insulating layer (Figure 3A). Figure 3B shows an AFM image of an NTFET device composed of an individual semiconducting SWNT.[7] When a semiconductor and a metal are brought into contact, a potential barrier develops at the interface because of the mismatch in work functions;[15] the interfacial potential barrier is typically referred to as a Schottky barrier (SB). In NTFET devices, the height of the SB at the CNT–contact interface depends on the work function of the metal (Figure 3C),[4] where a larger work-function mismatch will result in a larger SB. Under a constant S–D bias voltage (V_{SD}) the conductance of semiconducting CNTs can be modulated by applying a potential to the gate electrode, denoted here as V_G. The applied V_G serves to modify the SB and therefore the probability of a hole (h^+) traveling from the metal contact into the CNT valence band. Sweeping V_G between positive and negative voltages under a constant bias will produce a transfer characteristic I–V_G (Figure 3D), where the CNT conductance is shown to depend on the metal work function of the device contact.

NTFETs are adept at monitoring molecular environments, because the CNT conduction channel is composed almost entirely of surface atoms, and even small changes in the local chemical environment will result in measurable changes in the device conductance. For example, semiconducting CNTs are p-type under ambient conditions.[12,13] Therefore electron donation into the valence band will result in charge-carrier (h^+) recombination, causing a decrease in conductance and a shift in the transfer characteristic curve I–V_G towards more negative voltages. Conversely, electron withdrawal will serve to increase the hole concen-

Alexander Star was born in Almaty, Kazakhstan, in 1971. He immigrated to Israel in 1991, where he received a B.S. degree in chemistry in 1994 and a Ph.D. in supramolecular chemistry (with Prof. Benzion Fuchs) from Tel Aviv University in 2000. He then spent two years as a postdoctoral associate in Prof. J. Fraser Stoddart's California NanoSystems Institute group at the University of California, Los Angeles. After his postdoctoral studies he was employed as Senior Scientist at Nanomix, Inc. for three years, working on the development of sensor applications of carbon nanotubes. He has been an Assistant Professor of Chemistry at University of Pittsburgh since 2005. His research interests are in molecular recognition at the nanoscale and nanotechnology-enabled molecular sensing.

Douglas R. Kauffman graduated with a B.S. in chemistry from the University of Pittsburgh in 2004. He remained at the University of Pittsburgh to pursue a Ph.D. with the Department of Chemistry under the guidance of Prof. Alexander Star, where he studies the design of nanomaterial-based electronic devices and chemical sensors. Currently investigating the optical spectroscopy and electronic properties of single-walled carbon nanotubes under chemical interaction, he is interested in developing new ways to monitor and control events occurring at the nanotube surface.

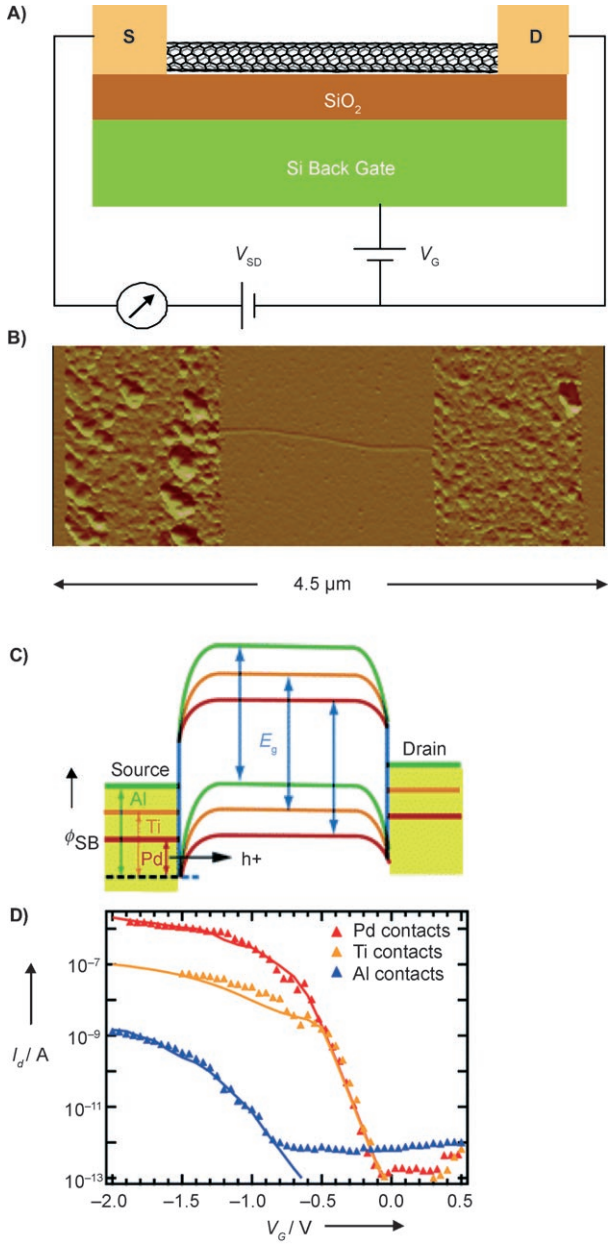

Figure 3. A) Schematic diagram of a nanotube field-effect transistor (NTFET) device with a semiconducting SWNT (black) contacted by two Ti/Au electrodes (light brown) representing the source (S) and the drain (D) with a Si back gate (green) separated by a SiO_2 insulating layer (dark brown) in a transistor-configured circuit. B) AFM image of a typical NTFET device with individual SWNTs connecting S and D electrodes; adapted from reference [7]. C) Diagram showing the Schottky barrier (SB) at the SWNT–metal-contact interface. The work-function mismatch between a semiconducting SWNT and metal creates a work-function-dependent SB. D) Transfer characteristic of NTFET devices composed of semiconducting SWNTs contacted by metals of different work functions operated at a bias $V_{SD} = -0.5$ V; adapted from reference [4].

tration in the CNT, leading to an increase in conductance and a shift in the transfer characteristic (I–V_G) towards more positive voltages. Adsorbing species can also reduce the CNT charge mobility by introducing scattering sites. This phenomenon results in a change in the slope of the transfer characteristic (dI/dV_G),[16] called the transconductance.[13] Lastly, because NTFETs behave as SB transistors,[17] they show extreme sensitivity to the work function of the device contact,[4] and chemical interaction with the device contact can serve to modify the SB at the CNT–metal interface. SB modification can produce a device response that is very similar to charge transfer with the CNT, and it can create ambiguity over the signal transduction mechanism of NTFET devices.

2. Carbon Nanotube Based Environmental Sensors

To date CNTs have shown sensitivity towards such gases as NH_3, NO_2, H_2, CH_4, CO, SO_2, H_2S, and O_2. Subsequently, efforts have been made to exploit these sensitivities in the development of new sensor technologies.

2.1. Ammonia (NH_3) and Nitrogen Dioxide (NO_2)

The ability to accurately monitor the concentrations of NH_3 and NO_2 in the air is important, because both chemicals adversely affect human and environmental health. Ammonia is primarily a concern in areas of high agricultural activity, because it is a natural waste product of livestock, but industrial sources include the manufacturing of basic chemicals, metals, textiles, and paper products as well as automotive emissions.[18] High levels of NH_3 can result in irritation to the eyes and respiratory tracts of humans and can negatively impact wildlife, livestock, and agricultural health.[19] NO_2 is also a potentially toxic gas that can lead to respiratory symptoms in humans and detrimentally influence the growth of agriculture.[20] Furthermore, atmospheric concentrations of either gas can lead to the creation of ground-level smog and acid rain. The threshold limit value (TLV), defined as the level of exposure that the typical worker can experience without an unreasonable risk of disease or injury, for NO_2 has been set as a time-weighted concentration (over a ten-hour day) of 3 ppm and at 25 ppm for NH_3 exposure.[21] Currently, metal oxide semiconductor (MOS) and solid electrolyte (SE) sensors are used for the detection of NO_2 and NH_3 gases.[22] Typical detection limits for commercial solid-state sensors range from 1–1000 ppm at an operating temperature of a few hundred degrees Celsius.[18,22] These types of sensors are inexpensive and robust, that is, they do not require much maintenance and have relatively long lifetimes. However, they do suffer from selectivity problems, because other oxidizing or reducing gases can produce sensor response.

In 2000 Dai and co-workers demonstrated the potential of CNT-based gas sensors when they reported the response of NTFET devices to NO_2 and NH_3 gases.[23] NTFET devices, utilizing a single semiconducting SWNT as the conduction channel, showed unique response to NH_3 and NO_2 through chemical gating of the SWNT. For example, Figure 4 A shows that NH_3 exposure resulted in a shift in the transfer characteristic gate voltage of approximately -4 V, while NO_2 exposure created a shift of approximately $+4$ V. Alternatively, when the NTFET device was held at a constant gate voltage of $V_G =$

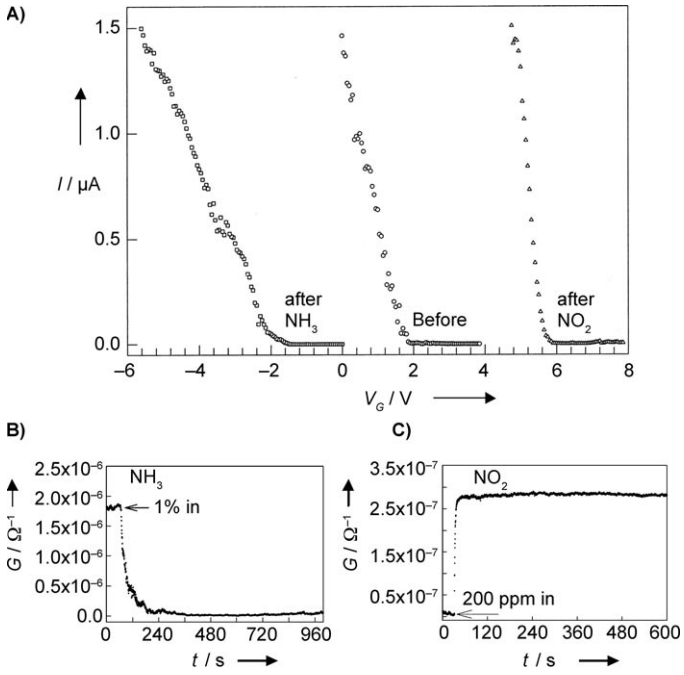

Figure 4. A) Response of an NTFET device with a single semiconducting SWNT as the conduction channel to NH_3 and NO_2 gas. B, C) Response of NTFET device at $V_G = 0$ V to 1% NH_3 (B) and at $V_G = +4$ V to 200 ppm NO_2 (C); adapted from reference [23].

0 V, exposure to NH_3 resulted in a decrease in current (Figure 4B), while NO_2 exposure ($V_G = +4$ V) resulted in an increase in device current (Figure 4C). The response time, defined as the time from sample introduction until signal stabilization, of the NTFET devices to 200 ppm NO_2 was a few seconds, and the sensitivity, defined as the resistance after exposure divided by the initial resistance, was approximately 100–1000. Recovery was slow at room temperature (ca. 12 h) but was decreased to approximately 1 h upon heating. The response time to approximately 1% NH_3 was a few minutes with a sensitivity between 10 and 100.

The effects of NO_2 exposure were explained by the removal of electronic density from the SWNT at a rate of approximately 0.1 electrons per adsorbed NO_2 molecule. However, the device response to NH_3 remained unclear, because calculations indicated no binding energy between the gas molecule and the SWNT. The authors suggested NH_3 may have indirectly influenced the SWNT electronic structure through interaction with hydroxy groups on the SiO_2 substrate, leading to partial neutralization of negative charges, or through interaction with other molecules adsorbed on the SWNT. Interestingly, the response of metallic SWNTs to these gases was much smaller, possibly because small changes in the density of states near the Fermi level did not substantially affect the charge-carrier density in metallic SWNTs.

A floodgate of interest in the development of CNT-based sensors was generated by this initial report of CNT gas sensing. Subsequently, a substantial portion of papers reporting gas-phase chemical interaction with CNTs for the purpose of sensor development has focused on NO_2 and NH_3. While these two gases represent important environmental pollutants, they also present an interesting fundamental challenge, because the nature of their interaction with CNTs is still unclear. While many regard NH_3 and NO_2 to be the prototypical electron-donating and electron-withdrawing species, respectively, disagreement still exists over the exact mechanism of their interaction with CNTs and the nature of CNT-based sensor response.

2.1.1. *Mechanism of NO_2 and NH_3 Interaction with CNTs*

Several groups have conducted theoretical investigations into the interaction between CNTs and NO_2 or NH_3. However, a general consensus on the nature of the interaction has yet to be realized. For example, Peng and Cho[24] detailed the electronic structure of the SWNT, the NO_2 molecule, and

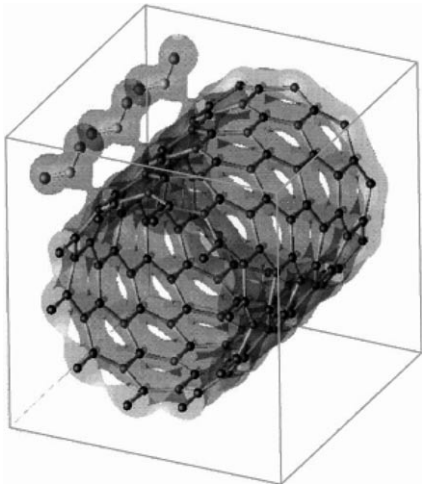

Figure 5. Valence electron density plot showing NO_2 molecules adsorbing onto a (10,0) semiconducting SWNT.[24]

the combined SWNT–NO_2 system (Figure 5). The experimental results obtained by Dai and co-workers[23] were validated by showing that there was zero binding affinity with NH_3 and that the NO_2 lowest unoccupied molecular orbital (LUMO) resided energetically lower than the SWNT valence band edge, thus allowing electron transfer from the SWNT into the NO_2 molecule.

Using DFT calculations, Lee and co-workers[25] reported that gas adsorption on SWNTs results in a withdrawal of approximately 0.1 electrons per NO_2 molecule and a donation of 0.04 electrons per adsorbed NH_3 molecule from the SWNT valence band. The calculated charge transfer upon NH_3 adsorption is in disagreement with the Dai[23] and Cho[24] groups, who suggested a mechanism other than charge transfer was responsible for device response to NH_3 gas. Zhao et al.[26] used self-consistent field (SCF) electronic structure calculations to determine that gas molecules can diffuse through SWNT bundles and absorb in interstitial sites; this claim is supported by findings from the Johnson group.[27] Furthermore, they concluded that 0.061–0.089 electrons are withdrawn from SWNTs upon NO_2 adsorption and 0.027–0.033 electrons are donated into the SWNT upon NH_3

adsorption. Similarly, the Maiti group[28] used DFT to calculate the binding affinities of NH_3 at defect sites on SWNTs. They reported charge transfer from the NH_3 molecule to the SWNT varying from 0.025–0.176 electrons per adsorbed NH_3 molecule. These results suggest that charge transfer is the major contributor to conductivity changes in CNT-based devices.

Using a self-consistent charge density-functional-based tight-binding (SCC-DFTB) method, the Lee group reported that NO_2 adsorption is more favorable on metallic SWNTs.[29] However, this result disagrees with theoretical findings by the Lin,[30] Li,[31] Baushlicher,[32] and Dai[33] groups, who have all calculated nonzero charge transfer between semiconducting SWNTs and NO_2 molecules. Furthermore, these groups have determined that chemisorption, rather than physisorption, is the dominant interaction, thus providing a possible explanation for long recovery times from NO_2 exposure. It should be noted that Baushlicher and co-workers[32] claimed that chemisorption of NO_2 is not likely to be responsible for the observed changes in CNT conductance and suggested that further investigation is necessary.

As with theoretical reports, there are discrepancies among the experimental evidence of NO_2 and NH_3 interaction with CNTs. For example, a combined theoretical and experimental investigation using CNT devices was reported by Santucci et al.,[34] who concluded that NO_2 adsorption onto the sidewalls of SWNTs led to the formation of a new state near the SWNT Fermi level; the formation of this new electronic state is the proposed mechanism for device response. Similar modification of the CNT Fermi level was found for NO_2[35] and NH_3[36] adsorption. Goldoni et al.[37] showed SWNT sensitivity to NO_2 and NH_3 using core-level photoemission spectroscopy under ultra-high-vacuum conditions, and later studies by Valentini et al.[38,39] suggested NO_2 chemisorption may occur at CNT defect sites, which others have claimed may lead to the formation of NO[40] and/or NO_3.[41] The Borguet[42a] and Snow[42b] groups, using IR spectroscopy and a combined electronic and theoretical approach, respectively, both concluded that SWNT defects play a crucial role in SWNT analyte sensitivity.

Larciprete et al. reported that NO_2 decomposition occurs on rhodium-decorated[43] and contacted[44] SWNTs, which suggests that device response may originate from SB modification through NO_2 interaction with the metal contacts. Furthermore, device behavior indicative of SB modification in NTFETs during NO_2 exposure was found by the Barbara group[45] using devices with polymer-passivated contacts and by the Hara group[46] using devices with Al contacts. Interestingly, Bradley et al.[47] reported device response to NH_3 with SiO-passivated NTFET device contacts, and using their experimental data they calculated that NH_3 adsorption resulted in a donation of 0.04 electrons per molecule,[48] which is in perfect agreement with the value that Lee and coworkers calculated.[25] Similarly, Jones et al.[49] concluded that NTFET device response to NH_3 exposure resulted from charge transfer with the CNT.

2.1.2. NH_3 and NO_2 Sensors Based on CNTs

With the inconsistencies between theoretical and experimental reports, it is understandable why controversy exists over the mechanism of CNT sensor response. Despite the controversy over physisorption versus chemisorption and charge transfer versus SB modification, great strides have been made in the sensitivity and selectivity of CNT-based sensors for these species.

Several groups have focused on improving the response of sensors composed of CNT networks without any chemical functionalization. For example, Li et al.[50] reported 44-ppb detection of NO_2 with bare SWNTs dropcast onto interdigitated electrodes, and Santucci et al.[34] used CNT films grown on Pt substrates to show 10-ppb detection of NO_2 at 165 °C. Quang et al.[51] concluded that bare SWNTs can detect 5 ppm NH_3, saturate above 40 ppm, and suffer from memory effects (electronic signal resulting from irreversible analyte binding) after multiple exposures. Several reports emerged suggesting that improved sensor performance could be realized with increased operation temperature[52a–d] or by subjecting the device to centrifugal force.[52e] Furthermore, Valentini et al.[53] reported that the cross sensitivity between NH_3 and NO_2 of CNT-based sensors could be reduced through oxidation in air, and Penza et al.[54] reported improved sensitivity to NO_2 and NH_3 using Co catalyst islands for CNT growth in sensor devices.

Multiple research groups have explored varying sensor architectures in the effort to design more sensitive devices. For example, Ong et al.[55] developed a wireless passive sensor for NH_3 detection based on a planar inductor–capacitor design utilizing MWNTs, and Chopra et al.[56] reported a CNT-based resonant-circuit sensor that showed slower NH_3 response but better recovery than more conventional resistance-based CNT sensors. Jung et al.[57] reported a CNT sensor for detecting gases adsorbed onto the surface of the inner walls by growing them in alumina templates; this approach resulted in well-ordered and aligned CNTs that showed high sensitivity to NO_2 and NH_3.

Decoration of CNTs with metal or semiconducting particles can increase sensitivity and selectivity. For example, we have reported[58] that metal-decorated (including Pd, Pt, Rh, and Au) SWNT NTFET devices can be used in a sensor array for the detection of NO_2 and NH_3, among other gases (see below). Lu et al. reported the fabrication of a 32-element sensor utilizing pristine, polymer-decorated, and metal-decorated (Pd, Au) SWNT devices that could differentiate between NO_2, HCN, HCl, Cl_2, acetone, and benzene.[59] Penza et al. reported that Au- and Pt-decorated CNTs demonstrated a response ($\Delta R/R_0$) to NO_2 and NH_3 that was approximately six to eight times larger than that of pristine CNTs.[60] They explained that the increased sensitivity was due to a spillover effect at the metal nanoparticles.

MOS–CNT composites have also found use in NO_2 and NH_3 sensors. For example, Liang et al.[61] reported a low-resistance gas sensor composed of SnO_2-coated CNTs that showed ppm sensitivity to NO_2, and Bittencourt et al.[62] demonstrated that WO_3 films impregnated with CNTs showed sensitivity to 500 ppb NO_2 under ambient conditions

and 10 ppm NH_3 at 150 °C, far below the typical operating temperature of WO_3 sensors. The detection mechanism was explained in terms of modification of SBs present at the grain boundaries between WO_3 particles. Similarly, Hoa et al.[63] showed that SWNT–SnO_2 demonstrates room-temperature sensitivity to 10 ppm NH_3.

The best sensitivity to NH_3 and NO_2 has been found in CNT–polymer composites. For example, the Haddon group functionalized SWNT NTFET devices with the polymer poly(*m*-aminobenzene sulfonic acid) (PABS).[64] The SWNT–PABS devices showed n-type behavior and significant sensitivity to 5 ppm NH_3 owing to PABS deprotonation during NH_3 exposure (Figure 6). This deprotonation resulted

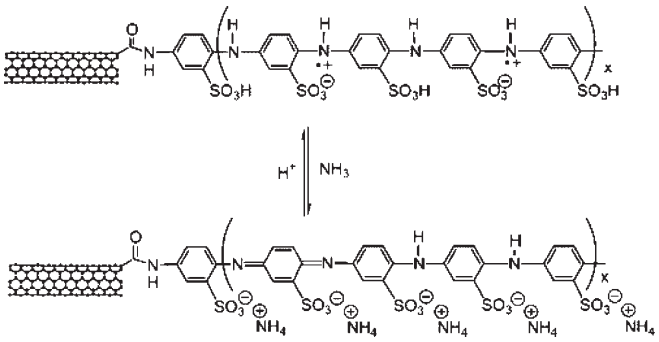

Figure 6. Proposed NH_3 sensing mechanism of the SWNT–PABS complex.[64]

in hole depletion from the SWNT and a reduction in the overall conductance of the SWNT–PABS system. Building upon this work, Zhang et al.[65] used SWNT–PABS devices to reach detection limits of 100 ppb NH_3 and 20 ppb NO_2 with short response time and total recovery. The response of the SWNT–PABS sensor to NO_2 was explained through protonation of the PABS polymer, which is logically the opposite of the mechanism described for NH_3 detection. Furthermore, Li et al.[66] reported the fabrication of a poly(methyl methacrylate) (PMMA)-functionalized SWNT sensor for NH_3 detection that was free of the effects of relative humidity.

The lowest detection limit for NO_2 (100 ppt) was realized by the Dai group using poly(ethylene imine) (PEI)-coated SNWT devices (Figure 7 A).[67] Furthermore, the application of a nafion coating (a polymeric perfluorinated sulfonic acid ionomer) allowed selective NH_3 detection in the presence of NO_2 by blocking the adsorption of NO_2 on the SWNT surface. Lastly, a report by Zhang et al.[68] detailed the electrochemical functionalization of SWNTs with the polymer polyaniline (PANI), as shown in Figure 7 C. This SWNT–PANI system achieved the detection limit of 50 ppb for NH_3 (Figure 7 D). Remarkably, both the SWNT–PEI and SWNT–PANI systems showed fast and complete recovery and to date serve as examples of the most sensitive CNT-based sensor platforms for NO_2 and NH_3 detection.

Theoretical calculations suggested the possibility of using atomically doped CNTs for sensing purposes. For example, doping CNTs with boron or nitrogen would effectively result in hole or electron doping, respectively.[69,70] This doping scheme is interesting, because it would allow the reactivity of

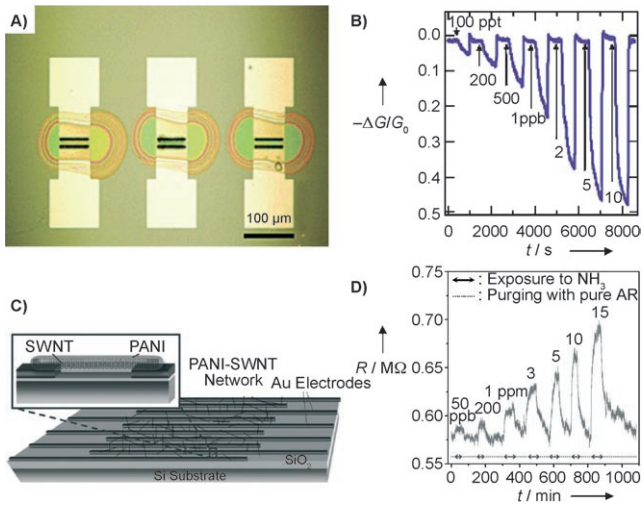

Figure 7. A) Photograph of SWNT devices coated with PEI; B) their response to differing concentrations of NO_2, expressed as the relative change in conductance $-\Delta G/G_0$ at zero gate voltage; adapted from reference [67]. C) Schematic depiction of the SWNT–PANI sensing element; D) its response to varying concentrations of NH_3; adapted from reference [68].

the CNT to be tailored towards a certain species of analyte. This approach has been used by Villalpando-Páez et al.[71] in the design of an NH_3-sensitive device utilizing nitrogen-doped CNTs (N-CNTs). They reported that the N-CNT sensors demonstrated response times on the order of a few tenths of a second and reached a steady state value in 2–3 s. They attributed this quick response to gas interaction at the nitrogen sites on the CNT sidewall. The authors speculate that higher doping concentrations may yield far more sensitive devices.

2.2. CNT-Based Hydrogen (H_2) and Methane (CH_4) Sensors

The risk of explosion is the primary reason for accurate measurement of H_2 and CH_4 levels, because concentrations as low as 4% in air can become explosive.[21] Typically, H_2 is detected using MOS sensors with incorporated Pd metal.[22] The first H_2 MOS sensor was reported in 1975[72] and consisted of a MOS field-effect transistor (MOSFET) with a Pd gate electrode. SE sensors have also found commercial success in the detection of H_2 gas.[22] CH_4 is a colorless, odorless gas that, under the correct circumstances, can displace O_2 and cause asphyxiation or become explosive. It is therefore vitally important to monitor this gas in enclosed environments, such as mining operations. Moreover, CH_4 is a much more powerful greenhouse gas than CO_2; it can originate from such sources as landfills, fossil fuel production sites, and agricultural areas. MOS and SE sensors are commonly used for the detection of CH_4.[22]

Bare CNTs do not show appreciable sensitivity to H_2, so efforts have been made to find a suitable functionalization scheme to decorate CNTs with H_2-sensitive materials. The Dai group first reported the sensitivity of Pd-decorated SWNTs to ppm levels of H_2 gas.[73] SWNT devices were coated

with a thin (ca. 5-Å) coating of Pd by electron beam evaporation, which led to the formation of Pd nanoparticles on the SWNT sidewall. Upon exposure to concentrations of 40 and 400 ppm H_2, the conductance of the Pd-decorated SWNTs decreased, yielding a response time of a few seconds; full recovery was observed after approximately 400 seconds. The sensing and recovery mechanisms were described as follows: H_2 dissociates into atomic hydrogen on the Pd surface at room temperature; this decreases the Pd work function and leads to electron donation into the SWNT. Once H_2 gas is removed from the system, O_2 molecules react with the atomic hydrogen to produce H_2O, returning the system, and the SWNT conductance, to its original state.

Soh and co-workers[74] reported a microelectronic diode that consisted of a thin layered Pd/CNT/Si structure and showed sensitivity towards exposure to 100% H_2 environments. Sayago et al.[75] demonstrated sensors that were composed of SWNTs spray cast onto Al substrates and functionalized with Pd nanoparticles; these sensors showed completely reversible detection of 0.5–0.3% H_2. Figure 8A

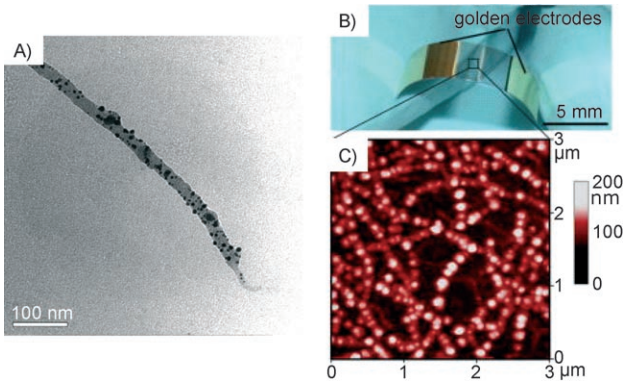

Figure 8. A) TEM image of a Pd-decorated SWNT bundle.[75b]. B) Photograph of the flexible Pd–SWNT H_2 sensor. C) An AFM image of the Pd-decorated SWNT network that serves as the H_2 sensing element and conduction channel; adapted from reference [80a].

shows a transmission electron microscopy (TEM) image of a Pd-decorated SWNT bundle.[75b] The bare SWNTs showed H_2 sensitivity above 200 °C, and SWNTs chemically functionalized with Pd nanoparticles showed a H_2 response (ΔR) approximately 43 times greater than SWNTs sputter coated with Pd.[75b]

Rinzler and co-workers reported the fabrication of a CNT film-based H_2 sensor that demonstrated a room-temperature detection limit of approximately 10 ppm and consumed only about 0.25 mW power.[76] They found that thinner (7-nm vs. 25-nm) SWNT films subjected to thermally evaporated Pd (as opposed to sputter-coated) showed better response to H_2. The reasons for the enhanced H_2 sensor response of thermally coated versus sputter-coated SWNTs remained unclear but may have resulted from damage caused during the sputtering process. Moreover, they suggested that the thinner films responded better because of a better association between the SWNTs and Pd. Dag et al.[77] conducted a theoretical study on the adsorption of H_2 on bare and Pt-decorated SWNTs, and Kumar and Ramaprabhu[78] later demonstrated the sensitivity of Pt-decorated MWNTs to 4% H_2 at various temperatures. Mubeen et al.[79] reported on the influence that the electrochemical deposition parameters (potential and charge) had on the sensitivity of Pd–SWNT-based sensors to ppm concentrations of H_2. We have found that SWNTs electrochemically decorated with Pt, Pd, and Rh showed strong response to H_2 gas.[58] Lastly, Sun and Wang[80] used electrochemically Pd-decorated SWNTs to create a flexible hydrogen sensor (Figure 8B) that had ppm sensitivity, complete recovery, and excellent reproducibility after more than 1000 cycles. Figure 8C is an AFM image of the Pd-decorated SWNT network that served as the H_2-sensitive element and sensor conduction channel.

Ding et al.[81] showed reversible, room-temperature detection of ppm concentrations of H_2 with a sensor consisting of vertically aligned CNTs grown in an Al template with a Pd top gate (Figure 9). Cusano et al.[82] took an entirely different

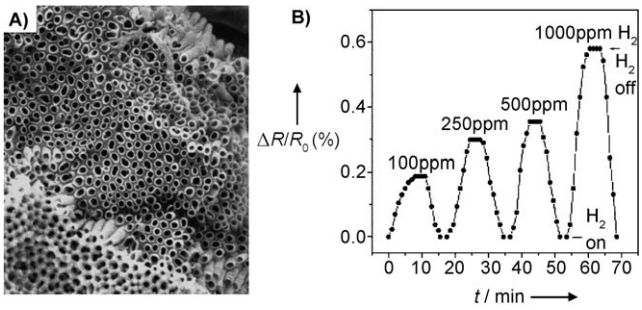

Figure 9. A) Aligned CNT array grown in an Al template. B) Response to H_2 exposure expressed as the relative change in device resistance $\Delta R/R_0$ at zero gate voltage; adapted from reference [81].

approach when they reported the fabrication of an optical-fiber-based sensor for H_2 detection at cryogenic temperatures. It is important to monitor cryogenically cooled H_2 in rocket engines, but Pd-based sensors are unable to dissociate H_2 at very low temperatures. Thus, an optical probe was developed that relied on H_2 adsorption modifying the SWNT film thickness, dielectric constant, and reflectance. Using this approach they were able to detect H_2 concentrations of 1–4% at 113 K.

The detection of CH_4 with CNT-based sensors has not experienced as much popularity as H_2 detection, but a few studies have been reported. For example, adsorption of CH_4 onto SWNTs has been calculated to result in a donation of approximately 0.025 electrons per adsorbed molecule,[26] but experimental confirmation of this conclusion has been difficult.[58] Lu et al.[83] reported the fabrication of a CH_4 sensor based on Pd-decorated SWNTs that demonstrated sensitivity to 6–100 ppm in room-temperature air. The authors suggested that upon gas exposure a weakly bound $Pd^{\delta+}(CH_4)^{\delta-}$ complex is formed, thus increasing the conductance of the Pd–SWNT network. The lack of CNT-based sensors for the detection of CH_4 is an indication that further study into the fundamental interactions between this gas and functionalized CNTs is needed.

2.3. CNT-Based Carbon Monoxide (CO) Sensors

The accurate measurement of environmental CO levels is important, because CO is a gas produced by incomplete hydrocarbon burning and accompanies almost all combustion processes. CO is especially dangerous, because with no odor or color it is undetectable by humans, it becomes explosive at concentrations above 12%, and has a TLV of 25 ppm.[21] Environmentally, a major source of CO emissions is vehicle exhaust, which adds to the formation of smog. Currently the leading sensor technologies for detection of this gas are MOS and SE sensors.[22]

Theoretical[24] and experimental[34] reports suggest that CO does not engage in charge transfer with bare SWNTs; however, Matranga and Bockrath[84] suggested that CO adsorbs by hydrogen bonding with hydroxy groups on the CNT that formed as a result of purification steps. Additional theoretical studies suggest CNT-based CO sensors could be constructed using radially deformed CNTs[85] and CNTs doped with atoms such as boron and nitrogen[86] or aluminum.[87]

Even though CO gas does not engage in charge transfer with bare CNTs, reports have emerged of CNT-based sensors that rely on detection mechanisms other than charge transfer. For example, Varghese et al.[88] reported a CNT device that could detect the presence of CO through capacitive changes. While this device functioned reversibly, the authors only reported response in the presence of 100% CO. Chopra et al.[89] reported the detection of CO gas through changes in the resonant frequency of CNT films. Resonant-frequency sensors operate on the principle that gas adsorption will modify the dielectric constant of the substrate and theoretically could demonstrate CO detection limits in the ppb regime.[90] Functionalized CNTs have shown good CO sensitivity, as reported by Wanna et al.[91] with a PANI-functionalized CNT sensor capable of reversible response to CO from 100–500 ppm, and by Bittencourt et al.[62] in their report of 10-ppm CO detection with WO_3 films impregnated with CNTs. Moreover, we have shown that Pt- and Rh-decorated SWNTs show strong response ($\Delta G/G_0 \gtrsim 0.7$) to a concentration of 2500 ppm CO gas.[58]

2.4. CNT-Based Sulfur Dioxide (SO_2) and Hydrogen Sulfide (H_2S) Sensors

Accurate detection of SO_2 and H_2S is important for environmental and safety reasons. SO_2 is a reactive gas that primarily originates from human activities such as coal combustion and petroleum refining. SO_2 is environmentally harmful, because it can aid in the formation of acid rain; furthermore, it can induce respiratory problems in humans and has a TLV of 2 ppm.[21] H_2S is dangerous gas because of its flammability and toxicity; it has a lower explosive limit (LEL) of 4% and a TLV of 10 ppm.[21] The accumulation of H_2S emissions is a serious concern for petroleum refineries and coke ovens. Currently, MOS and SE sensors are employed for the detection of these two sulfur-containing gases.[22]

Experimentally, SO_2 has been shown to adsorb onto bare CNTs[92] with an effect similar to NO_2.[37,41] However, reports of CNT-based sensors for this gas are scarce. Interestingly, Suehiro et al.[93] reported CNT sensitivity to SO_2, but gas exposure resulted in device behavior consistent with electron-donating species. It was unclear why SO_2 acted as an electron-donating molecule in this scenario, and no further explanation was provided. Lastly, in our report of a metal-decorated SWNT sensor array, we were able to detect 50 ppm H_2S in air with Pd-decorated SWNTs.[58] The lack of reports detailing the development of CNT-based sensors for the detection of SO_2 and H_2S suggests further investigation into the interactions between CNTs and SO_2 and H_2S is needed.

2.5. CNT-Based Oxygen (O_2) Sensors

SE sensors have found great commercial success as oxygen sensors,[22] specifically in monitoring the oxygen concentration in automobile exhaust. These types of sensors demonstrate excellent longevity at high operational temperatures; however, they are also sensitive to other oxidizing gases. A major challenge that CNT-based sensors face is the current inability to operate as oxygen sensors. Zettl and co-workers have shown that oxygen dramatically effects the physical properties of CNTs.[94,95] However, debate surrounds exactly how CNT-based devices respond to O_2 gas. For example, Avouris and co-workers reported that device response to O_2 stems from interaction at the SWNT–metal-contact interface, resulting in a modification of the device SB.[96] Debate continues, because some experimental evidence suggests that O_2 adsorption does affect the CNT electronic structure,[37,94,97] and theoretical treatments of the system have resulted in varying adsorption energies and predicted charge transfer.[24,26,98] Despite the controversy over how O_2 adsorption influences the CNT electronic structure, solid experimental evidence shows that O_2 desorption at room temperature, even under high vacuum, is considerably too slow for sensor applications.[94,95,97] While some recent efforts have improved the room-temperature desorption of O_2 to a few hundred seconds,[99] the technique still required a vacuum system and therefore would not be an appropriate setup for a realistic sensor design. Using a surface acoustic wave (SAW) device based on a CNT thin film, Chopra et al. could detect the presence of O_2 based on resonant-frequency shifts. This approach showed a response time (the time from sample introduction until signal stabilization) of approximately 10 min, but it was not chemically selective.[89] It is apparent that considerable future effort will be needed for the development of a usable CNT-based solid-state O_2 sensor.

2.6. CNT Sensor Arrays

Table 1 summarizes the gases that CNT-based sensors have been successful at detecting. A challenge faced by all solid-state sensors, including those based on CNTs, is analyte selectivity. An interesting approach to the problem of sensor selectivity is the idea of sensor arrays in which multiple

Table 1: Summary of CNT–gas interactions for the development of environmental sensors; the detection limit is given for each particular analyte.[a,b]

Analyte	CNT Material/Method	Detection Limit	References
NO_2	calculation	N/A	[24–26, 29–33]
	bare CNTs	10 ppb[a] [34]	[23, 34, 35, 37–41, 43–46, 50, 52–54]
	vertically aligned CNTs	25 ppb	[57]
	metal-decorated CNTs	100 ppb[a] [60]	[58–60]
	metal oxide decorated CNTs	500 ppb[62]	[61, 62]
	polymer-coated CNTs	100 ppt[67]	[65, 67]
NH_3	calculation	N/A	[25, 26, 28]
	bare CNTs	5 ppm[51]	[23, 36, 37, 42, 47–49, 51–54]
	vertically aligned CNTs	5 ppm[a]	[57]
	CNT capacitor	N/A	[55]
	CNT resonant frequency sensor	ca. 10 ppm	[56]
	metal-decorated CNTs	5 ppm[a] [60]	[58–60]
	metal oxide decorated CNTs	5 ppm[a] [63]	[62, 63]
	polymer-coated CNTs	100 ppb[65]	[64–68]
	atomically doped CNTs	ca. 1 %[a]	[71]
H_2	Pd-decorated CNTs	10 ppm[a] [76]	[58, 73–76, 79, 80]
	Pt-decorated CNTs	0.4 %[a] [58]	[58, 77, 78]
	vertically aligned CNTs	100 ppm	[81]
	cryogenically cooled CNT optical probe	4 %[a]	[82]
CH_4	calculation	N/A	[26]
	metal-decorated CNTs	6 ppm[83]	[58, 83]
CO	calculation	N/A	[24]
	bare CNTs	100 ppm[a] [34]	[34, 84]
	metal-decorated CNTs	2500 ppm[a] [58]	[58]
	metal oxide decorated CNTs	10 ppm[a]	[62]
	radially deformed CNTs	N/A	[85]
	atomically doped CNTs	N/A	[86, 87]
	CNT capacitor	N/A	[88]
	CNT resonator frequency sensor	1500 ppm[a] [90]	[89, 90]
	polymer-coated CNTs	167 ppm[a]	[91]
SO_2	bare CNTs	10 ppm[a] [93]	[37, 41, 92, 93]
H_2S	metal oxide decorated CNTs	50 ppm[a]	[58]
O_2	calculation	N/A	[24, 26, 98]
	bare CNTs	N/A	[37, 94–97, 99]
	CNT SAW sensor	1500 ppm[a] [90]	[89, 90]

[a] If the sensor detection limit was not explicitly provided in the original report, then the lowest tested analyte concentration is listed. [b] For this group of gases, MOS- and SE-type sensors dominate the commercial sensor market and typically demonstrate detection limits in the ppm range.

sensing elements, each decorated with a particular material, are used simultaneously. The combined response of each element is then used to make an analyte-specific response pattern that can selectively determine the response to a particular analyte. We have used this approach with metal-decorated NTFET devices to detect various gas-phase analytes.[58] Figure 10A depicts the individual responses of many metal-decorated NTFET devices in our sensor array. While each metal did not display total selectivity for a particular analyte, the combined response of many devices can create an analyte-specific pattern, which we used to recognize NO_2, NH_3, H_2, CO, and H_2S. Figure 10B is an optical image accompanied by corresponding scanning electron microscopy (SEM) images of several metal-decorated NTFET devices. Figure 10C depicts the principal component analysis (PCA) of the sensor array response to various analytes. Each analyte has a specific pattern when plotted in 3D space; in this way sensor arrays can discriminate between different analytes. We have recently shown that charge transfer between metal-decorated CNT devices and gas molecules is dependent upon potential barriers at the CNT–metal-nanoparticle interface,[100] which may help explain response in metal-decorated CNT sensor array devices.

Lu et al.[59] reported the design of a sensor array consisting of 32 sensing elements including pristine, polymer-decorated, and metal-decorated CNTs that could differentiate between NO_2, HCN, HCl, Cl_2, acetone, and benzene. CNT technology has the potential to excel in the design of arrays, because the inherently small size of CNT devices will allow for the integration of large numbers of functionalized CNT sensor elements that would show unique response to numerous species.

2.7. Comparison to Other State-of-the-Art Methods: Advantages and Challenges to CNT Sensor Use

Currently, MOS and SE gas sensors hold a majority of the commercial market for the gases discussed thus far. These two types of sensors have found commercial success in the industrial gas sensor market because they are relatively inexpensive to fabricate, they show good sensitivity and accuracy, and they are suitable for monitoring ppm concentrations of gaseous analytes at high temperatures. However, while the MOS sensor is easily portable, stable, durable, and shows fast response time, it suffers from a low selectivity towards analyte species. SE sensors demonstrate better analyte selectivity; however, they suffer from poor stability and durability, they can demonstrate sluggish response time, and they are not well suited for portable devices.[22] The fundamentals and operation of MOS and SE sensors has been thoroughly covered in the literature[22] and they will only be used here for comparison to CNT-based sensor operation.

A major difference between current MOS and SE and CNT-based sensors is the operating temperature. MOS and

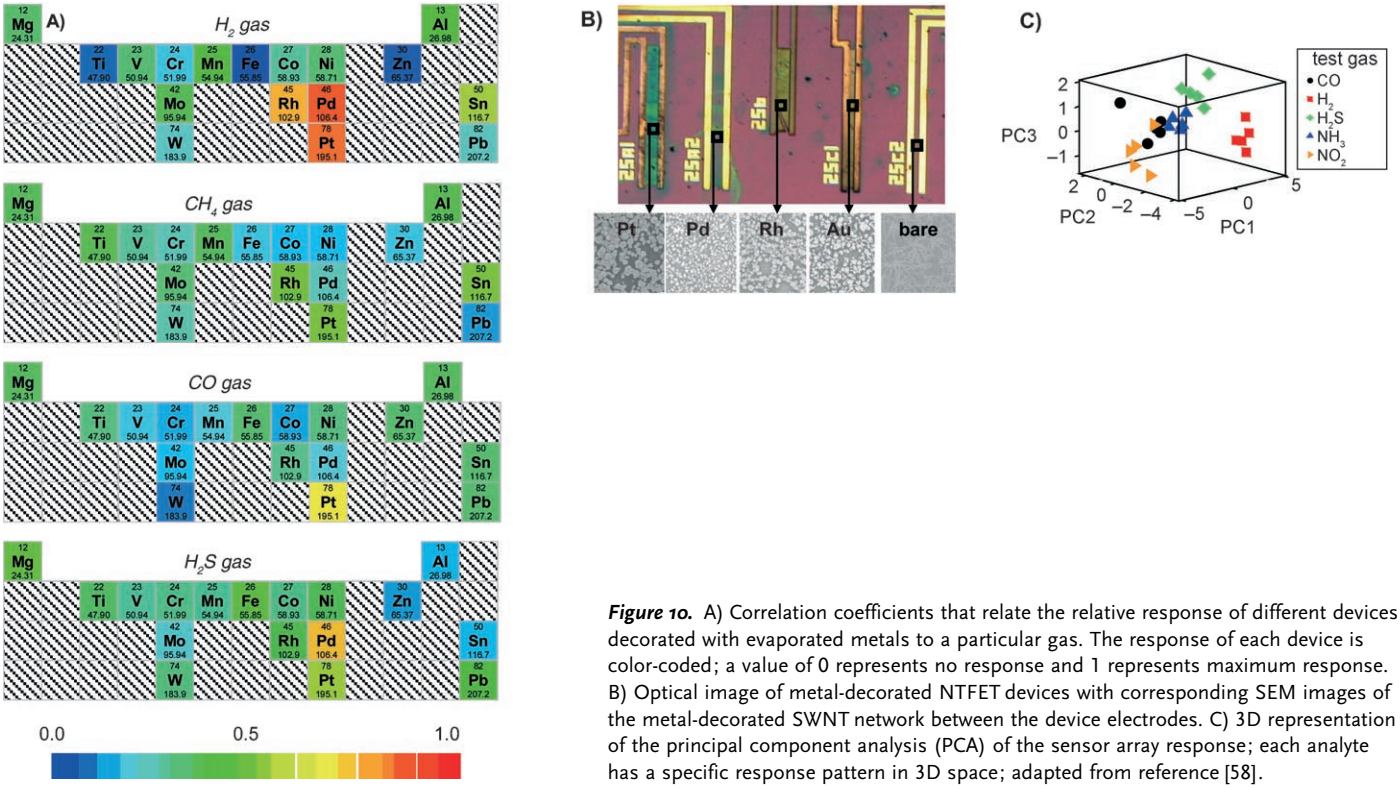

Figure 10. A) Correlation coefficients that relate the relative response of different devices decorated with evaporated metals to a particular gas. The response of each device is color-coded; a value of 0 represents no response and 1 represents maximum response. B) Optical image of metal-decorated NTFET devices with corresponding SEM images of the metal-decorated SWNT network between the device electrodes. C) 3D representation of the principal component analysis (PCA) of the sensor array response; each analyte has a specific response pattern in 3D space; adapted from reference [58].

SE sensors often operate at temperatures between several hundred to over 1000 °C, whereas CNT-based sensors show effective analyte sensitivity at room temperature. The ability of CNT sensors to operate in low-temperature regimes is an advantage for several reasons. First, it is an intrinsic safety advantage, because it reduces the risk of explosion in the presence of combustible gases. For example, typical MOS sensors require explosion-proof housings if they are to be used for detecting combustible gases because of the potential sparking hazard associated with the device heating elements. Secondly, CNT-based sensors will not be as sensitive to temperature fluctuations as MOS and SE sensors. If an MOS or SE sensor is subjected to a slight draft, perhaps created by a swinging door or air conditioning unit, the temperature-based resistance of the device will change.[22] This is especially problematic in very small sensors in which heat loss can occur through both the heating and the interrogation wires. Furthermore, a major concern for both MOS and SE sensors is degradation after long periods of operation at elevated temperature, because it can lead to changes in surface structure and irreversible binding of analyte molecules. The effect of such changes on the sensor resistance is termed "drift" and is a crucial limitation to the sensor lifetime.[22] Additionally, SE sensors face the problem of increased electronic conductivity at high temperatures,[22] which is a potential source of error. Lastly, MOS and SE sensors require an uninterrupted power source, and once a device has lost power it will give false positives until it has reached its optimum operational temperature. The ability to operate CNT-based sensors at room temperature is inherently safer in environments with combustible gases, it reduces the sensitivity to minor temperature fluctuations and thermally induced drift, and it decreases the overall power consumption of the device.

One disadvantage of room-temperature operation is the potential interference from relative humidity. CNT devices show sensitivity to H_2O vapor, but the exact influence on the CNT electronic structure is still under debate, and differing opinions include electronic donation into the CNT,[101] hydrogen bonding with oxygen defect sites on the CNT,[102] and the introduction of charge-trapping sites on the CNT through direct H_2O adsorption and/or interaction with the SiO_2 substrate.[103] Regardless of this debate, several groups have developed humidity sensors containing CNTs,[104] $LiClO_4$-doped CNTs,[105] polymer-functionalized CNTs,[106] CNT–biomolecule complexes,[107] as well as CNT-based capacitor,[108] field-ionization,[109] and quartz-crystal microbalance (QCM) sensors.[110] The sensitivity to water is a challenge that researchers need to consider when designing sensor architectures using CNTs.

Because studies have yet to address the suitability of CNT-based sensors for extended operation at elevated temperatures, it is impossible to speculate on their potential for applications in the automotive or processing arenas. However, the room-temperature operation and low power consumption of these devices suggests more potential for personal safety and network sensor applications. For example, the intrinsic ease at which CNTs can be incorporated into microscale electronics will facilitate the fabrication of tiny sensor devices for ultraportable and wearable sensor technology. The low power consumption of these devices will result in extended sensor lifetime using current battery

technology. When coupled to wireless technology, such devices could form a complete sensor network that could monitor an entire structure for potentially harmful analytes.

3. Carbon Nanotube Based Medical Sensors

The medical industry typically relies on laboratory instruments for diagnostic purposes. However, there is a substantial potential for portable diagnostic devices. While these types of medical sensors may lack the exquisite sensitivity of methods such as GC-MS or spectroscopy, they would provide a fast and accurate tool for first responders to quickly assess the status of a patient. Because they demonstrate such extreme environmental sensitivity and allow for incorporation into very small, low-power electronic devices, CNTs are uniquely suited for the development of portable first-response medical diagnostic tools.

3.1. CNT-Based Carbon Dioxide (CO_2) Sensors

The ability to monitor CO_2 is important for personal safety and medical reasons. At levels above 5% CO_2 becomes toxic. The measurement of CO_2 concentrations in human breath, called capnography, currently utilizes nondispersive infrared (NDIR) sensors.[111] The use of NDIR CO_2 sensors is advantageous, because they demonstrate extraordinary long-term stability, accuracy, and have low power consumption. Furthermore, the measurement of a strong CO_2 absorption wavelength reduces interference, and this type of sensor can easily measure low-ppm-range CO_2 concentrations.[112a] Today this type of technology has even been incorporated into portable systems for pre-hospital care by first responders;[112b] however, their high cost inhibits general use.

Zhao et al.[26] reported that CO_2 adsorption should result in a net transfer of approximately 0.015 electrons into the CNT per adsorbing molecule, but this has yet to be shown experimentally. Varghese et al.[88] noted cross sensitivity to CO_2 with their impedance-based CNT gas sensors, which showed a lower detection limit of approximately 10% CO_2 (10^5 ppm). Ong et al.[55,113] reported on the development of a wireless passive CNT-based gas sensor that demonstrated sensitivity to CO_2. By placing a thin layer of a CNT–SiO_2 composite on a planar inductor–capacitor resonant circuit, they were able to detect varying concentrations of CO_2 by monitoring the permittivity of the CNT composite. Their setup allowed measurement of CO_2 concentrations of 0–100% under varied relative humidity and temperature with a response time of approximately 45 s. Additionally, Zribi et al.[89b] were able to accurately measure 0–15% CO_2 with a CNT-based resonator-frequency sensor. Their sensor design allowed a lower detection limit of approximately 1% CO_2 (10000 ppm).

We have shown that NTFETs functionalized with a polymer matrix consisting of PEI and starch demonstrate excellent sensitivity to CO_2.[114] The response to CO_2 exposure was a reversible decrease in device conductance that scaled linearly with the CO_2 concentration. We concluded that the response originated as a possible combination of the following two mechanisms: 1) CO_2 reaction with the polymer composite reduced the overall electron-donating character of the PEI; 2) structural changes in the starch complex introduced charge-scattering sites on the SWNT. While this device responded well to CO_2 with a dynamic operating range between 500 ppm and 10% CO_2 in air, PEI is sensitive to other acidic gases, specifically NO_2 and SO_2, and would inevitably show cross-sensitivity if these species were present.

3.2. CNT-Based Nitric Oxide (NO) Sensors

The detection of NO in medical patients is important, because changes in NO levels can be indicative of certain ailments such as Alzheimer's or asthma.[115] The ability to monitor NO levels in patients' breath is advantageous for medical professionals trying to make diagnostic assessments. Currently, chemiluminescence is commonly used for the detection of NO gas in a patient's breath.[116] While this technique is extraordinarily sensitive, with a detection limit of 300 ppt, the required instrumentation is large, expensive, and needs various supporting accessories, such as vacuum pumps and an ozone generator.

Long and Yang reported that CNTs adsorb oxides of nitrogen, including NO, in the presence of O_2.[92] The ability to adsorb a medically relevant chemical species such as NO in the presence of O_2 presents the opportunity for the creation of a medical sensor; however, the literature is sparsely populated with reports of CNT–NO interactions. We have found that bare SWNT networks demonstrate little response to NO gas, but once they are decorated with metal nanoparticles (Pt, Pd, Au, Ag) they show unique electronic characteristics under a NO atmosphere.[100] Liang et al.[61] reported cross sensitivity to NO with their CNT–SnO_2-based sensor. The device design is illustrated in Figure 11A; the CNT–SnO_2 composite was dropcast onto a cylindrical ceramic tube with an internal heating element. At 300°C this device detected NO concentrations between 2 and 50 ppm (Figure 11B).

Lastly, we have developed a NO sensor based on PEI-functionalized SWNT networks for detecting NO gas in simulated breath conditions for asthma diagnosis.[117] In this report, NO was oxidized into NO_2 with a CrO_3 converter, and the converted NO_2 then reacted with the PEI layer on the SWNT network (Figure 11C). We were able to detect 5-ppb concentrations of converted NO in pure N_2 (Figure 11D), and using an ascarite scrubber to remove CO_2 we were able to detect 15 ppb NO in simulated breath—a realistic requirement for detecting exhaled NO for asthma monitoring.

3.3. CNT-Based Ethanol (EtOH) Sensors

The detection of EtOH in is an essential measurement for law enforcement officials that needs to be conducted in the field with quick, accurate, and reproducible results. The breathalyzer, the most common technique for EtOH analysis, relies on redox chemistry between EtOH and $K_2Cr_2O_7$ and has a lower detection limit of 0.001% blood alcohol

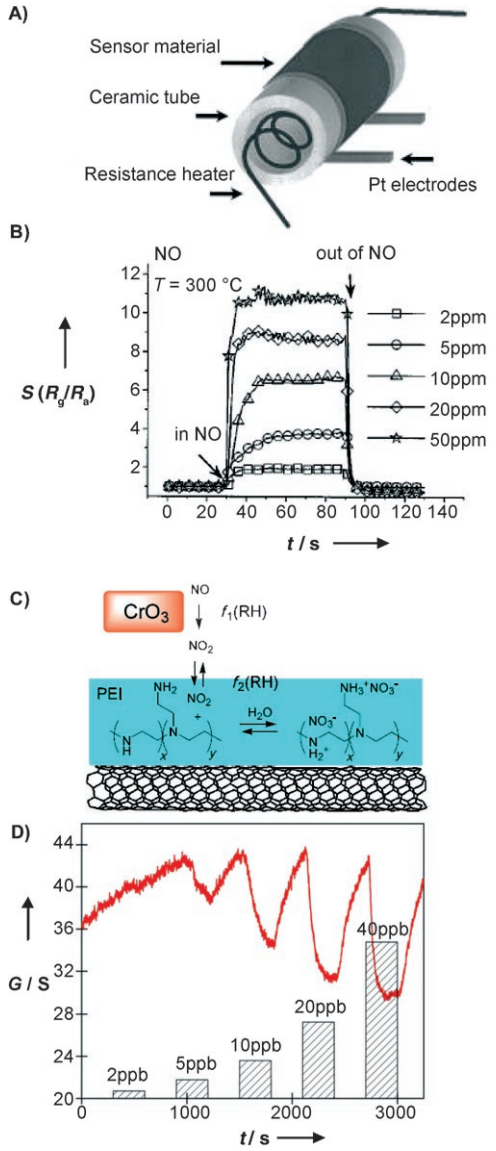

Figure 11. A) Sensor design with a CNT–SnO_2 composite coating a ceramic cylinder with an internal resistive heating element. B) Sensor response to NO gas at 300 °C, expressed as the relative change between the device resistance under gas exposure (R_g) and in air (R_a); adapted from reference [61]. C) Mechanistic diagram of the conversion of NO to NO_2 using a CrO_3 converter and detection with PEI-coated SWNTs. D) Response of the PEI-coated SWNTs to NO gas under N_2 with a 5-ppb detection limit; adapted from reference [117].

content.[118] Methods utilizing the IR absorbance of EtOH are also available,[119] and these offer the same advantages as NDIR CO_2 sensors in terms of performance and reliability. NDIR-based sensors have the ability to accurately monitor concentrations of EtOH in blood at 0.0049 %, well below the legal limit of most jurisdictions. However, the optical sensors are inherently more complicated and expensive, which limits their general use.

Iijima and co-workers first reported on the adsorption of alcohol vapors onto SWNTs.[120] They concluded that the purification process increased the microporosity and oxygen functionality of SWNTs, leading to a greatly enhanced adsorption of MeOH and EtOH on the SWNT sidewall at 303 K. Someya et al.[121] used NTFET devices composed of isolated SWNTs to monitor the concentration of EtOH down to approximately 300 ppm. Exposure to pure alcohol vapors resulted in a substantial decrease in device conductance that was reproducible over 55 individual runs. The authors explained the device response in terms of the alcohol either doping the SWNT or interacting with the SiO_2 substrate and filling charge traps. The authors do concede, however, that either of the above mechanisms could serve to indirectly modify the device SB at the SWNT–metal contact, and they suggested further investigation was needed to fully understand device response.

In their report on the cross sensitivity of CNT films to various gases and vapors, Cantalini et al.[122] reported substantial device response to 500 ppm EtOH at 165 °C under dry N_2 and 80 % relative humidity, where EtOH exposure resulted in a sharp increase in resistance. Penza et al.[123] described the operation of a SAW sensor that was fabricated by spray casting CNT solutions onto quartz substrates and coating them with SiO_2. The EtOH concentration was measured by monitoring changes in the resonant frequency of the device during analyte adsorption. They claimed a theoretical detection limit of 1.3 ppm EtOH at room temperature but experimentally realized a detection limit of 3.9 ppm.

Villalpando-Páez et al.[71] reported a strong yet reversible response to EtOH with vertically aligned nitrogen-doped CNTs that showed a response time of under one second. Wei et al.[124] reported that vertically aligned CNT–poly(vinyl acetate) films showed reversible sensitivity to EtOH and MeOH. Interestingly, they found that the selectivity of the sensor to certain vapors could be modified by changing the composition of the polymer composite. Penza et al.[125] reported several examples of CNT sensors based on resonant frequency and reflectivity changes upon analyte absorption for the detection of EtOH and MeOH as well as other organic vapors (see below). By detecting vapor adsorption with two unique transduction mechanisms (change in resonant frequency and reflectivity), the authors suggest that this type of technology could be used to develop multitransducer and multisensor arrays for the analysis of complicated chemical samples. Liang et al.[61] described sensitivity to EtOH between 10 and 1000 ppm with their SnO_2-coated CNT devices, while Wisitsoraat et al.[126a] concluded that the EtOH sensitivity and response time of SnO_2 films was greatly increase with the inclusion of CNTs. Liu et al.[126b] reported sensitivity towards EtOH and liquid petroleum gas with SnO_2-decorated MWNTs, and Chen et al.[127] reported sensitivity to 10 ppm EtOH vapors with CNT–SnO_2 core–shell nanostructures that showed reversible operation at 300 °C and long-term stability.

3.4. CNT-Based Organic-Vapor Sensors

In 1971 Pauling et al. reported that hundreds of organic vapors exist in the exhaled breath of humans.[128] Later it was shown by Gordon et al.[129] that these organic vapors could be used to identify lung cancer patients. Organic vapors in human breath are also symptomatic of diabetes, sleep apnea,

infection, sickle cell disease, asthma, breast cancer, chronic obstructive pulmonary disease, several types of liver disease, kidney failure, and cystic fibrosis.[130]

Santhanam et al.[131] reported a chemical vapor sensor composed of poly(3-methylthiophene)-functionalized CNTs that showed sensitivity to different chloromethanes. Interestingly, this sensor did not respond to CH_4, acetone, acetaldehyde, benzaldehyde, THF, MeOH, or EtOH. The authors explain the selectivity of this sensor with the ability of the polymer to accept only halogenated species. As mentioned previously, the CNT-based resonator/optical sensor reported by Penza et al.[125] was sensitive to various organic vapors including isopropyl alcohol, acetone, ethyl acetate, and toluene, and Wei et al.[124] demonstrated that vertically aligned CNT–poly(vinyl acetate) films also showed reversible sensitivity to hexane, THF, cyclohexane, acetone, $CHCl_3$, ethyl acetate, MeOH, toluene, DMF, and CCl_4.

Ma et al.[132] reported that polyaniline composites containing CNTs demonstrated fast and reversible room-temperature response to trimethylamine, triethylamine, NH_3, and HCl. The authors described the sensing mechanism in terms of protonation or deprotonation of the polyaniline polymer, which led to a subsequent increase or decrease, respectively, in measured current upon vapor exposure. They found that increased amounts of CNT in the polymer composite actually reduced the sensitivity to trimethylamine vapors; this effect was attributed to the strong electronic interaction between the CNTs and polyaniline polymer, which increased the polymer conductivity but reduced the overall gas sensitivity of the composite. Sánchez et al.[133] reported a combined experimental and theoretical investigation of a sensor composed of CNTs embedded in a sol–gel-derived TiO_2 matrix that showed fast room-temperature response to and recovery from acetone vapor and NH_3. The TiO_2–CNT composite showed improved sensitivity and demonstrated n-type behavior upon acetone and NH_3 exposure. The authors explained the acetone response through the formation of a negatively charged ion at the TiO_2 cluster but conceded that further investigation is necessary to understand the n-type NH_3 response. Lastly, a theoretical paper by Wang et al.[134] suggested that boron-doped SWNTs could serve as formaldehyde-sensitive devices. They showed, using local density approximations, that formaldehyde adsorption on pristine SWNTs resulted in a donation of 0.021–0.039 electrons, but adsorption on boron-doped SWNTs could result in electron donation as high as 0.121 electrons. The authors suggest this type of doped SWNT could act as a new medical sensor with high intrinsic sensitivity for formaldehyde vapor.

3.5. Comparison to Other State-of-the-Art Methods: Advantages and Challenges to CNT Sensor Use

Currently, hospital analysis of medically relevant gases and vapors is typically done with GC-MS, solid-state MOS sensors, spectroscopy, or electrochemical techniques.[22,135] With the exception of breath analysis for EtOH concentrations and blood O_2 monitoring with optical probes,[22] these techniques require large, costly, and sophisticated equipment. Clinical diagnostic techniques typically employ sample preconcentration in breath-component analysis owing to the low concentration (ppt to ppb) of the analyte of interest;[135] this procedure limits the speed of the diagnosis, but it results in unrivalled sensitivity and analyte discrimination. Because CNT technology is intrinsically suited for miniaturization, it may find acceptance in the medical field as the basis for inexpensive disposable sensors. This type of medial device could be applied in routine clinical tests, take-home medical testing devices, or as portable tools for first-response medical diagnostics.

Table 2 summarizes the reported CNT-based materials used for sensing medically relevant gases and vapors. Because of the small size and relatively inexpensive fabrication of CNT devices, it may be possible for first responders to perform an initial medical diagnosis on a patient on the way to the hospital. In this situation, reproducibility and speed may outweigh absolute sensitivity, as the medical technician will need to make fast judgments to stabilize the patient.

Another possible application of CNT-based sensor technology could be personal diagnostic tools for home use, where increased vapor or gas concentrations in exhaled breath could signal to the patient that a medical condition is worsening and appropriate medical precautions should be taken. We have shown it is possible to use CNT-based technology to develop sensors capable of measure low concentrations of CO_2[114] and NO[117] in human breath; future developments will hopefully yield robust, inexpensive, and accurate devices for preliminary or at-home medical diagnosis.

4. Carbon Nanotube Based Sensors for Military and Defense Applications

With the increased threat of terrorist activity, there is an unfortunate need for the detection of chemical vapors indicative of malicious intent. For the detection of explosives, nitrotoluene and 2,4-dinitrotoluene (DNT) have been used for the development of 2,4,6-trinitrotoluene (TNT) sensors. Furthermore, cyclotrimethylenetrinitramine, commonly known as RDX, and ethylene glycol dinitrate (EGDN) are components commonly found in military-grade explosives. Towards the development of sensors for chemical warfare agents (CWAs), specifically nerve agents, simulants are often used: dimethyl methylphosphonate (DMMP) for sarin, diiso-

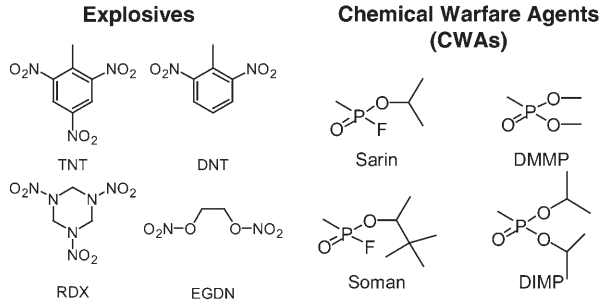

Figure 12. Structures of some common chemicals used for explosives and chemical warfare agent sensor testing.

Table 2: Summary of CNT–gas and vapor interactions for the development of medical sensors, providing a comparison to the detection limits of typical commercially available sensors.[a]

Analyte	Current methods	Detection Limit	CNT material/method	Detection Limit[b]	References
CO_2	spectroscopic	low ppm	calculation	N/A	[26]
			bare CNT impedance	10%	[88]
			CNT capacitor	20%[a][113]	[55,113]
			PEI/starch-coated CNTs	500 ppm	[114]
			CNT resonator	ca. 1%	[89b]
NO	spectroscopic	300 ppt	bare CNTs	10 ppm[a]	[100]
			metal-decorated CNTs	10 ppm[a]	[100]
			SnO_2-decorated CNTs	2 ppm[a]	[61]
			PEI-functionalized CNTs	5 ppb	[117]
EtOH	breathalyzer ($K_2C_2O_7$, redox)	10 ppm	bare CNTs	ca. 300 ppm[a][121]	[120–122]
			CNT-based SAW Sensor	1.3 ppm	[123]
	spectroscopic	49 ppm	CNT resonant frequency sensor	1.1 ppm[125b]	[125]
			metal oxide decorated CNTs	10 ppm[a][60,127]	[61,126,127]
			polymer-coated CNTs	N/A	[124]
			nitrogen-containing CNTs	N/A	[71]
organic vapors	GC-MS	ppt to ppb[c]	CNT resonant frequency sensor	ppm	[125]
			polymer-functionalized CNTs	4 ppm[a][131]	[124,131,132]
			TiO_2-decorated CNTs	N/A	[133]

[a] If the sensor detection limit was not explicitly provided in the original report then the lowest tested analyte concentration is listed. [b] A concentration of 1% corresponds 1×10^4 ppm. [c] With analyte preconcentration.

propyl methylphosphonate (DIMP) for soman, and thionyl chloride ($SOCl_2$) for nerve-agent precursors. Figure 12 displays the structures of some common chemicals used in sensor development for military applications. Currently a large array of commercial technology is available for the detection of explosives and CWAs,[136,137] and these are summarized in Table 3.

Several groups have made efforts towards developing CNT-based sensors for explosives and nerve agents. For example, Li et al.[50] reported a detection limit of 262 ppb for 3-nitrotolune using bare SWNTs dropcast onto interdigitated electrodes. Novak et al.[138] reported the selective sub-ppb detection of DMMP using SWNT-based sensors. Their approach is interesting, because they took the typical SWNT-based NTFET device design (Figure 13A,B) and incorporated it into a compact flow cell (Figure 13C). SWNTs were grown directly onto the inner wall of the quartz flow cell, and silver paint was used to create contacts at either end; typical resistances for the chemiresistor flow cells was between 1–10 MΩ. Using this design, they demonstrated sensitivity to 1 ppb DMMP (Figure 13D).

The slow response and recovery of the devices suggests that the signal may be a cumulative effect of irreversible analyte adsorption, and some have argued that this is an

Table 3: Summary of CNT–gas and vapor interactions for the development of military and defense sensors providing a comparison to the detection limits of typical commercially available sensors.[a]

Analyte	Current Methods	Detection Limit	CNT Material	Method	Detection Limit	References
explosives	canine detection	ca. 1 ppb	bare CNTs	chemiresistor	262 ppb	[50]
	IMS[b]	ppm		capacitor	ppm[a]	[143]
	ECD[c]	ppm	DNA-functionalized CNTs	chemiresistor	<1 ppm	[142]
	SAW sensor[d]	ppm				
	GC-MS	ppb to ppm				
	spectroscopy	ppb to ppm				
CWAs	detection paper	$\mu g\,cm^{-2}$	bare CNTs	chemiresistor	<1 ppb	[138]
	gas-detection tube	ppm		capacitor	0.5 ppb	[143]
	FPD[e]	ppb to ppm	metallic CNTs	chemiresistor	700 ppb	[140]
	IMS	ppm	polymer-functionalized CNTs	flexible chemiresistor	25–50 ppm	[141]
	SAW	ppm	DNA-functionalized CNTs	chemiresistor	<1 ppm	[142]
	PID[f]	ppb to ppm				
	GC-MS	ppb to ppm				

[a] If the sensor detection limit was not explicitly provided in the original report then the lowest tested analyte concentration is listed. [b] Ion mobility spectrometry (IMS), [c] Electron capture detector (ECD). [d] Surface acoustic wave (SAW). [e] Flame photometric detector (FPD), [f] Photoionization detector (PID).

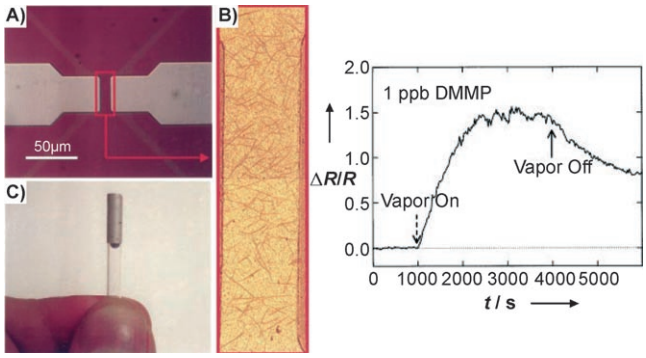

Figure 13. A) NTFET device composed of a network of SWNTs as the conduction channel. B) AFM image of the SWNT network between contacts. C) Chemiresistor flow cell sensor with SWNTs grown in the inner wall of the tube and Ag paint used as contacts. D) Response of the sensor to 1 ppb DMMP expressed as the relative change in resistance $\Delta R/R$; adapted from reference [138].

inappropriate way to describe the sensitivity and detection limit, because SWNT sensors that exploit irreversible binding have a potentially infinitely small detection limit.[139] The only technical limitation to the sensitivity would be the exposure time (at any concentration) required to absorb the requisite amount of analyte before signal transduction occurred. Regardless, the device showed strong initial response to 1 ppb DMMP (Figure 13D), which is an impressive sensitivity to such a low concentration of nerve-agent simulant.

Strano and co-workers employed devices composed of mostly metallic SWNTs ordered with alternating-current dielectrophoresis as chemical sensors for the detection of DMMP and $SOCl_2$.[140] By passivating the device contacts, they concluded that device response to $SOCl_2$ resulted from charge transfer with the SWNT, as confirmed by in situ Raman spectroscopy. Strong sensitivity to 50 ppm $SOCl_2$ was shown, and a complete and nearly immediate recovery was obtained by flushing the device with pulses of saturated water vapor at room temperature.

Cattanach et al.[141] reported the design of a flexible sensor for the detection of DMMP and DIMP. The sensor devices were composed of SWNT bundles deposited onto a polyethylene terephthalate (PET) polymer film. These devices demonstrated good sensitivity even under flexation and showed selectivity over high concentrations (10000 ppm) of interferent vapors such as hexane, xylene, and H_2O (contaminants that would be found in a battlefield situation from gasoline and diesel fuel combustion). Furthermore, selectivity for DMMP and DIMP was achieved through the use of a 2-μm layer of a the polymer polyisobutylene, where sensitivity to approximately 300 ppm DIMP was maintained in the presence of 30000-ppm concentrations of interferent gases. The authors suggest that this type of technology could be used to pattern flexible sensors of any design for the rapid determination of chemical warfare agents.

Johnson and co-workers took a unique approach to chemical vapor sensing in that they used DNA-functionalized SWNTs as the sensing element and conduction channel in NTFET devices.[142] In this way, they were able to detect chemical vapors that did not impact the conductivity of bare SWNTs. For example, the DNA-functionalized SWNT showed sensitivity towards propionic acid and trimethylamine. Furthermore, this sensor architecture responded to DMMP and DNT. The DNA-functionalized SWNT sensors showed fast response and recovery (seconds) and good reproducibility over 50 exposure cycles. The authors suggest that this type of SWNT hybrid could be used in the development of nanoelectronic "nose" and "tongue" sensors.

Snow et al.[143] reported on the design of chemical sensors that utilize changes in the SWNT capacitance ΔC rather than conductance ΔG. In addition to measuring the network conductance, their design also allows measurement of the capacitance between the Si substrate and SWNT network (Figure 14A). The electric field polarizes adsorbing molecules, which changes the device capacitance, thus allowing for

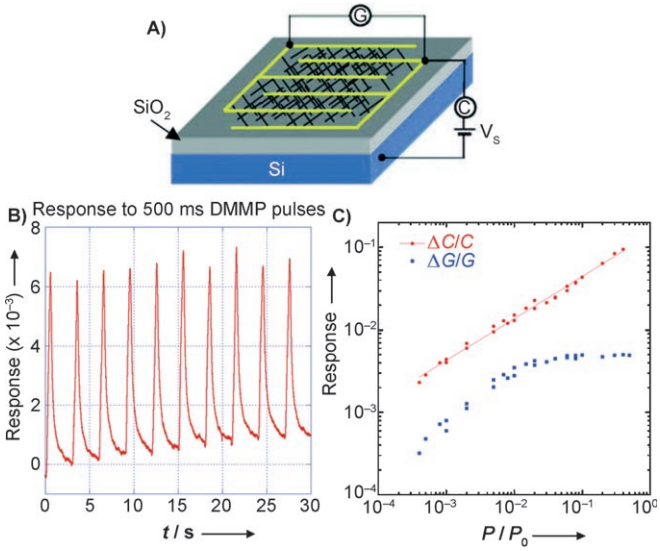

Figure 14. A) Schematic depiction of a SWNT sensor capable of measuring both conductance G and capacitance C. B) Capacitance response ($\Delta C/C_0$) of the SWNT sensor shown in part A to 500-ms pulses of DMMP delivered in air at $P = 0.0005\,P_0$. C) Comparison of the independent conductance ($\Delta G/G_0$) and capacitance response of the SWNT sensor as a function of acetone concentration. The conductance response saturates at approximately 0.01 P_0, while the capacitance response continues to increase; adapted from reference [143b].

accurate measurement of dilute vapor concentrations with fast and nearly complete sensor response, as shown in Figure 14B with the capacitance response ($\Delta C/C_0$) to dilute DMMP vapors in air. The authors claim that this technique can detect DMMP and DNT at sub-ppb levels, which is well below the capabilities of conventional sensors. Using capacitance to monitor chemical species has unique advantages in that it allows for the low-noise measurement of low-vapor-pressure analytes that would not engage in significant charge transfer with the SWNT and therefore not significantly alter the device conductance.

Mention should be made of the difference between the response of the capacitance-based (Figure 14B) and network chemiresistor (Figure 13D) sensors. Even a cursory exami-

nation of the two plots reveals that the capacitance-based sensor produces much sharper and reversible response peaks for the same analyte species. Moreover, the capacitance response does not show appreciable saturation during analyte exposure, as compared to the conductance response; this phenomenon is illustrated in Figure 14C with a comparison of the independent capacitance ($\Delta C/C_0$; red curve) and conductance ($\Delta G/G_0$; blue curve) response to varying acetone concentrations. An additional feature of this sensor architecture is that it provides the ability to perform simultaneous conductance and capacitance measurements, which gives a value $\Delta G/\Delta C$ that is unique for each analyte. The authors note that charge transfer can affect the capacitance of the SWNT sensor, but its effects on the capacitive response are small and only account for approximately 10% of the sensor response.

A final technique for detecting gases with low adsorption energy uses the field emission properties of CNTs, as reported by Kim.[144] This technique does not rely on charge transfer with the CNT, but rather monitors the electrons emitted from CNTs in the presence of analyte gas species. While these reports have only detailed operation in the presence of inert gases, the technique might be applicable to a variety of important species that do not engage in appreciable charge transfer with the CNT.

4.1. Comparison to Other State-of-the-Art Methods: Advantages and Challenges to CNT Sensor Use

Aside from laboratory techniques such as GC-MS and spectroscopy (IR, Raman, fluorescence, and chemiluminescence), there are currently several technologies available for the detection of trace explosives (Table 3).[136,137] With the exception of inexpensive detection paper and gas detection tubes, these commercially available units typically have good sensitivities with ppm-range detection limits, demonstrate response times on the order of seconds, and cost between $25000 and $50000. However, they often suffer from poor selectivity and strong analyte adsorption, and unless coupled with gas chromatographic (GC) capabilities (which increases the unit size and cost), they are used for the qualitative detection of explosive compounds.

Table 3 summarizes the development of CNT-based explosives and nerve-agent sensors as well as commercially available technologies. While the capability of incorporating most of these technologies into hand-held or portable units has facilitated the detection and screening of compounds indicative of explosives or CWAs, these sensors suffer from selectivity issues and are fairly expensive (several tens of thousands of US dollars per unit). CNT-based technologies have a potential for commercial service in this market because of their high sensitivity, extremely small size, and low cost of manufacturing. These unique traits suggest that instead of several conventional units surveying fixed locales, an entire sensor network could be developed in which many CNT-based sensors monitor ambient air for traces of explosives or CWAs. The small size will also allow for development of wearable sensors.

Another exciting possibility would be the development of so-called smart dust,[145] a wireless network of tiny battery-powered sensors distributed over a large area. By simply dispersing a vast number of these sensors over an area suspected of containing explosives or CWAs, the environment could be chemically mapped. This ability would allow military personnel to identify landmine fields and areas with CWA contamination without subjecting humans or canines to the potential dangers of manual searches. While current reports of CNT-based technologies for this purpose are promising, further work on sensor reproducibility and lifetime under real-life and battlefield conditions are needed before a definitive determination on their suitability can be made.

5. Conclusion and Outlook for Carbon Nanotube Based Sensors

CNTs are ideal nanomaterials for incorporation into solid-state sensor technologies, because they possess unique characteristics owing to their small diameter (several nanometers), while their relatively long length (several micrometers) enables efficient integration into electronic structures. Their exceedingly high aspect ratio and their high fraction of surface atoms enable CNTs to function as a highly sensitive detection layer and efficient conduction channel. CNT-based sensors have demonstrated sensitivity to a large number of gas- and vapor-phase analytes that are important in industrial, environmental, and personal safety and in medical and even military scenarios. Current efforts have led to devices with incredibly low detection limits and promising analyte selectivity. The broad range of sensitivities suggests that CNTs could serve as a platform technology for the development of sensors for many different environments.

In this early stage in CNT sensor technology it is hard to speculate on the future impact of CNT devices on the commercial sensor market. However, the largest potential for CNT-based sensor technology may reside in the development of sensor arrays and compact, low-power, portable sensors. Because CNTs can easily be incorporated into microscale electronic devices, it will be possible to create arrays with huge numbers of tiny sensing elements. This architecture will allow sensors to screen for multiple analytes simultaneously while maintaining a small instrumental footprint. Advances in the semiconductor industry will only serve to decrease the cost of device manufacturing, thus allowing for the commercialization of disposable sensors for a variety of personal safety or diagnostic applications. Furthermore, room-temperature operation of CNT sensors eliminates the need for internal heating elements and a continuous power supply. The low operating temperature will decrease thermally induced sensor aging, and the low power requirement will ultimately lead to longer sensor battery lifetime—two advantages over the current solid-state sensor technologies. Decreased manufacturing costs, combined with the incorporation of wireless technology, may allow the production of large wireless sensor networks for accurate chemical mapping of structures or large areas ("smart structures" or "smart dust").

While the field of solid-state chemical sensors is entering maturity, the inclusion of CNTs is only a recent development. In the few short years since the emergence of the first CNT-based chemical sensor there has been a tremendous effort to develop sensors for detecting important gaseous and vapor phase species in the field. However promising CNT-based sensor technology may seem, there are still fundamental challenges that need to be addressed before CNT devices can become viable candidates for commercial implementation. The current trend in the literature seems to direct more attention towards absolute detection limits rather than real-world applicability. While reports of low-ppb detection limits are becoming the standard for CNT-sensor papers, to date few reports detail long-term stability in environments in which conventional solid-state sensors have found success, such as dynamic environments with interfering species. This is not to say there is a lack of improvement in selectivity, as several excellent examples of species-specific response have been reported, but for CNT technology to become a viable alternative to current sensors, researchers need to demonstrate that CNT-based sensors can function in an environment outside of controlled laboratory conditions. The future of CNT-based sensor technology looks bright, and continued progress in this field will overcome the current challenges and lead to a class of sensor materials with superior sensitivity, reduced size, and extended lifetimes for a wide range of environments and applications.

Addendum

The field of CNT-based sensor research is progressing at a rapid pace, and since the acceptance of this manuscript many reports have emerged. We have selected a few examples to highlight; specifically, Haddon and co-workers[146] and our group[147] have reported on the simultaneous optical and electronic response of SWNT devices to gas- and vapor-phase analytes for a mechanistic tool to understand nanotube device response, and the Swager group[148] used polymer-modified SWNTs for the electronic detection of CWA simulants. Additionally, an entire issue of *Chemical Reviews*[149] has been devoted to new advances and current topics in modern chemical sensor technology.

A.S. would like to thank his co-workers from Nanomix Inc. cited in this article for their contribution to the research.

Received: September 28, 2007
Published online: July 18, 2008

[1] For an authoritative series of reviews on chemical sensor technology from 1988–1998, see: a) J. Janata, A. Bezegh, *Anal. Chem.* **1988**, *60*, 62R – 74R; b) J. Janata, *Anal. Chem.* **1990**, *62*, 33R – 44R; c) J. Janata, *Anal. Chem.* **1992**, *64*, 196R – 219R; d) J. Janata, M. Josowicz, D. M. Devaney, *Anal. Chem.* **1994**, *66*, 207R – 228R; e) J. Janata, M. Jasowicz, P. Vanysek, D. M. DeVaney, *Anal. Chem.* **1998**, *70*, 179R – 208R.

[2] Apart from CNTs, other emerging nanomaterials are used for sensing applications, for example metal and metal oxide nanoparticles in chemiresistor sensors: a) M. E. Franke, T. J. Koplin, U. Simon, *Small* **2006**, *2*, 36 – 50; for a review on nanowire-based biosensors, see: b) F. Patolsky, G. Zheng, C. M. Lieber, *Anal. Chem. A* **2006**, *78*, 4260 – 4269.

[3] G. Cao, *Nanostructures and Nanomaterials*, Imperial College Press, London, **2004**.

[4] Z. Chen, J. Appenzeller, J. Knoch, Y. M. Lin, P. Avouris, *Nano Lett.* **2005**, *5*, 1497 – 1502.

[5] S. Iijima, *Nature* **1991**, *354*, 56 – 58.

[6] For reviews on the application of CNTs to analytical science, see: a) M. Valcárcel, S. Cárdenas, B. M. Simonet, *Anal. Chem.* **2007**, *79*, 4788 – 4797; b) N. G. Portney, M. Ozkan, *Anal. Bioanal. Chem.* **2006**, *384*, 620 – 630; c) A. Merkoçi, *Microchim. Acta* **2006**, *152*, 155 – 156; for reviews on CNT-based chemical and physical sensors, see: d) N. Sinha, J. Ma, J. T. W. Yeow, *J. Nanosci. Nanotechnol.* **2006**, *6*, 573 – 590; e) J. R. Stetter, G. J. Maclay, *Adv. Micro Nanosyst.* **2004**, *1*, 357 – 382; f) J. Li in *Carbon Nanotubes* (Ed.: M. Meyyappan), Taylor and Francis, New York, **2005**, pp. 213 – 235; for an overview of CNT-based biological sensors, see: g) E. Katz, I. Willner, *ChemPhysChem* **2004**, *5*, 1084 – 1104; h) J. Wang, *Electroanalysis* **2005**, *17*, 7 – 14; i) Y. Lin, S. Taylor, H. Li, K. A. S. Fernando, L. Qu, W. Wang, L. Gu, B. Zhou, Y. P. Sun, *J. Mater. Chem.* **2004**, *14*, 527 – 541; j) K. Balasubramanian, M. Burghard, *Anal. Bioanal. Chem.* **2006**, *385*, 452 – 468; k) G. Grüner, *Anal. Bioanal. Chem.* **2006**, *384*, 322 – 335; for reviews on electrochemical CNT-based sensors, see: l) B. S. Sherigara, W. Kutner, F. D'Souza, *Electroanalysis* **2003**, *15*, 753 – 772; m) A. K. Wanekaya, W. Chen, N. V. Myung, A. Mulchandani, *Electroanalysis* **2006**, *18*, 533 – 550; n) G. G. Wildgoose, C. E. Banks, H. C. Leventis, R. G. Compton, *Microchim. Acta* **2006**, *152*, 187 – 214; o) F. W. Shan, J. S. Ye, *Mater. Tech.* **2004**, *19*, 11 – 12.

[7] B. L. Allen, P. D. Kichambare, A. Star, *Adv. Mater.* **2007**, *19*, 1439 – 1451.

[8] Special Issue: Carbon Nanotubes, *Acc. Chem. Res.* **2002**, *35*, 997 – 1113.

[9] For discussions on covalent and noncovalent CNT chemistry, see: a) J. L. Bahr, J. M. Tour, *J. Mater. Chem.* **2002**, *12*, 1952 – 1958; b) D. A. Britz, A. N. Khlobystov, *Chem. Soc. Rev.* **2006**, *35*, 637 – 659; c) D. Tasis, N. Tagmatarchis, A. Bianco, M. Prato, *Chem. Rev.* **2006**, *106*, 1105 – 1136; for discussions on the structure and electronic properties of CNTs, see: d) T. W. Odom, J. L. Huang, P. Kim, C. M. Lieber, *J. Phys. Chem. B* **2000**, *104*, 2794 – 2809; e) J. Bernholc, D. Brenner, M. B. Nardelli, V. Meunier, C. Roland, *Annu. Rev. Mater. Res.* **2002**, *32*, 347 – 375; f) E. Bekyarova, M. E. Itkis, N. Cabrera, B. Zhao, A. Yu, J. Gao, R. C. Haddon, *J. Am. Chem. Soc.* **2005**, *127*, 5990 – 5995; g) M. P. Anantram, F. Léonard, *Rep. Prog. Phys.* **2006**, *69*, 507 – 561; h) D. Aussawasathien, P. He, L. Dai, *ACS Symp. Ser.* **2006**, *918*, 246 – 268.

[10] S. Iijima, T. Ichihashi, *Nature* **1993**, *363*, 603 – 605.

[11] a) R. Saito, M. Fujita, G. Dresselhaus, M. S. Dresselhaus, *Appl. Phys. Lett.* **1992**, *60*, 2204 – 2206; b) K. Balasubramanian, M. Burghard, *Small* **2005**, *1*, 180 – 192.

[12] S. J. Tans, A. R. M. Verschueren, C. Dekker, *Nature* **1998**, *393*, 49 – 52.

[13] R. Martel, T. Schmidt, H. R. Shea, T. Hertel, P. Avouris, *Appl. Phys. Lett.* **1998**, *73*, 2447 – 2449.

[14] E. S. Snow, J. P. Novak, P. M. Campbell, D. Park, *Appl. Phys. Lett.* **2003**, *82*, 2145 – 2147.

[15] A. Zangwill, *Physics at Surfaces*, Cambridge University Press, Cambridge, **1988**.

[16] A. Star, J. C. P. Gabriel, K. Bradley, G. Grüner, *Nano Lett.* **2003**, *3*, 459 – 463.

[17] S. Heinze, J. Tersoff, R. Martel, V. Derycke, J. Appenzeller, P. Avouris, *Phys. Rev. Lett.* **2002**, *89*, 106801.

[18] B. Timmer, W. Olthius, A. van den Berg, *Sens. Actuators B* **2005**, *107*, 666 – 677.
[19] L. J. M. van der Eerden, P. H. B. de Visser, C. J. van Dijk, *Environ. Pollut.* **1998**, *102*, 49 – 53.
[20] K. Okano, T. Totsuka, *New Phytol.* **1986**, *102*, 551 – 562.
[21] Sigma–Aldrich Material Safety Data Sheets.
[22] a) M. J. Madou, S. R. Morrison, *Chemical Sensing with Solid State Devices*, Academic Press, New York, **1989**; b) *Chemical Sensor Technology, Vol. 1* (Ed.: T. Seiyama), Elsevier, New York, **1988**; c) N. Yamozoe, N. Miura, *MRS Bull.* **1999**, *24*, 37 – 43; d) J. W. Schwank, M. DiBattista, *MRS Bull.* **1999**, *24*, 44 – 48; e) Y. Shimizu, M. Egashira, *MRS Bull.* **1999**, *24*, 18 – 24; f) G. Korotcenkov, *Mater. Sci. Eng. B* **2007**, *139*, 1 – 23; g) J. W. Fergus, *Sens. Actuators B* **2007**, *122*, 683 – 693; h) D. D. Lee, D. S. Lee, *IEEE Sens. J.* **2001**, *1*, 214 – 224; i) R. Ramamoorthy, P. K. Dutta, S. A. Akbar, *J. Mater. Sci.* **2003**, *38*, 4271 – 4282.
[23] J. Kong, N. R. Franklin, C. Zhou, M. G. Chapline, S. Peng, K. Cho, H. Dai, *Science* **2000**, *287*, 622 – 625.
[24] S. Peng, K. Cho, *Nanotechnology* **2000**, *11*, 57 – 60.
[25] H. Chang, J. D. Lee, S. M. Lee, Y. H. Lee, *Appl. Phys. Lett.* **2001**, *79*, 3863 – 3865.
[26] J. Zhao, A. Buldum, J. Han. J. P. Lu, *Nanotechnology* **2002**, *13*, 195 – 200.
[27] W. Shi, J. K. Johnson, *Phys. Rev. Lett.* **2003**, *91*, 015504.
[28] J. Andzelm, N. Govind, A. Maiti, *Chem. Phys. Lett.* **2006**, *421*, 58 – 62.
[29] K. Seo, K. A. Park, C. Kim, S. Han, B. Kim, Y. H. Lee, *J. Am. Chem. Soc.* **2005**, *127*, 15724 – 15729.
[30] W. L. Yim, X. G. Gong, Z. F. Liu, *J. Phys. Chem. B* **2003**, *107*, 9363 – 9369.
[31] Y. Zhang, C. Suc, Z. Liu, J. Li, *J. Phys. Chem. B* **2006**, *110*, 22462 – 22470.
[32] A. Ricca, C. W. Baushlicher, *Chem. Phys.* **2006**, *323*, 511 – 518.
[33] S. Peng, K. Cho, P. Qi, H. Dai, *Chem. Phys. Lett.* **2004**, *387*, 271 – 276.
[34] S. Santucci, S. Picozzi, F. Di. Gregorio, L. Lozzi, C. Cantalini, L. Valentini, J. M. Kenny, B. Delley, *J. Chem. Phys.* **2003**, *119*, 10904 – 10910.
[35] L. Lozzi, S. Picozzi, I. Armentano, L. Valentini, J. M. Kenny, S. La Rosa, M. Coreno, M. De Simone, B. Delley, S. Santucci, *J. Chem. Phys.* **2005**, *123*, 034702.
[36] J. Kombarakkaran, C. F. M. Clewett, T. Peitraß, *Chem. Phys. Lett.* **2007**, *441*, 282 – 285.
[37] A. Goldoni, R. Larciprete, L. Petaccia, S. Lizzit, *J. Am. Chem. Soc.* **2003**, *125*, 11329 – 11333.
[38] L. Valentini, L. Lozzi, S. Picozzi, C. Cantalini, S. Santucci, J. M. Kenny, *J. Vac. Sci. Technol. A* **2004**, *22*, 1450 – 1454.
[39] L. Valentini, F. Mercuri, I. Armentano, C. Cantalini, S. Picozzi, L. Lozzi, S. Santucci, A. Sgamellotti, J. M. Kenny, *Chem. Phys. Lett.* **2004**, *387*, 356 – 361.
[40] F. Mercuri, A. Sgamellotti, L. Valentini, I. Armentano, J. M. Kenny, *J. Phys. Chem. B* **2005**, *109*, 13175 – 13179.
[41] A. Goldoni, L. Petaccia, L. Gregoratti, B. Kaulich, A. Barinov, S. Lizzit, A. Laurita, L. Sangaletti, R. Larciprete, *Carbon* **2004**, *42*, 2099 – 2122.
[42] a) X. Feng, S. Irle, H. Witek, K. Morokuma, R. Vidic, E. Borquet, *J. Am. Chem. Soc.* **2005**, *127*, 10533 – 10538; b) J. A. Robinson, E. S. Snow, Ş. C. Bădescu, T. L. Reinecke, F. K. Perkins, *Nano Lett.* **2006**, *6*, 1747 – 1751.
[43] R. Larciprete, S. Lizzit, L. Petaccia, A. Goldoni, *Appl. Phys. Lett.* **2006**, *88*, 243111.
[44] R. Larciprete, L. Pataccia, S. Lizzit, A. Goldoni, *J. Phys. Chem. C* **2007**, *111*, 12169 – 12174.
[45] J. Zhang, A. Boyd, A. Tselev, M. Paranjape, P. Barbara, *Appl. Phys. Lett.* **2006**, *88*, 123112.
[46] J. Suehiro, H. Imakiire, S. I. Hidaka, W. Ding, G. Zhou, K. Imasaka, M. Hara, *Sens. Actuators B* **2006**, *114*, 943 – 949.
[47] K. Bradley, J. C. P. Gabriel, A. Star, G. Grüner, *Appl. Phys. Lett.* **2003**, *83*, 3821 – 3823.
[48] K. Bradley, J. C. P. Gabriel, M. Briman, A. Star, G. Grüner, *Phys. Rev. Lett.* **2003**, *91*, 218301.
[49] F. E. Jones, A. A. Talin, F. Léonard, P. M. Dentinger, W. M. Clift, *J. Electron. Mater.* **2006**, *35*, 1641 – 1646.
[50] J. Li, Y. Lu, Q. Ye, M. Cinke, J. Han, M. Meyyappan, *Nano Lett.* **2003**, *3*, 929 – 933.
[51] N. H. Quang, M. V. Trinh, B. H. Lee, J. S. Huh, *Sens. Actuators B* **2006**, *113*, 341 – 346.
[52] a) C. Cantalini, L. Valentini, L. Lozzi, I. Armentano, J. M. Kenny, S. Santucci, *Sens. Actuators B* **2003**, *93*, 333 – 337; b) L. Valentini, I. Armentano, J. M. Kenny, C. Cantalini, L. Lozzi, S. Santucci, *Appl. Phys. Lett.* **2003**, *82*, 961 – 963; c) Y. T. Jang, S. I. Moon, J. H. Ahn, Y. H. Lee, B. K. Ju, *Sens. Actuators B* **2004**, *99*, 118 – 122; d) H. Q. Nguyen, J. S. Huh, *Sens. Actuators B* **2006**, *117*, 426 – 430; e) J. W. Lee, Y. Choi, K. J. Kong, J. O. Lee, H. Chang, B. H. Ryu, *Sens. Mater.* **2004**, *16*, 357 – 365.
[53] L. Valentini, C. Cantalini, L. Lozzi, S. Picozzi, I. Armentano, J. M. Kenny, S. Santucci, *Sens. Actuators B* **2004**, *100*, 33 – 40.
[54] M. Penza, G. Cassano, R. Rossi, A. Rizzo, M. A. Signore, M. Alvisi, L. Lisi, E. Serra, R. Giorgi, *Appl. Phys. Lett.* **2007**, *90*, 103101.
[55] K. G. Ong, K. Zeng, C. A. Grimes, *IEEE Sens. J.* **2002**, *2*, 82 – 88.
[56] S. Chopra, A. Pham, J. Gaillard, A. Parker, A. M. Rao, *Appl. Phys. Lett.* **2002**, *80*, 4632 – 4634.
[57] H. Y. Jung, S. M. Jung, J. Kim, J. S. Suh, *Appl. Phys. Lett.* **2007**, *90*, 153114.
[58] A. Star, V. Joshi, S. Skarupo, D. Thomas, J. C. P. Gabriel, *J. Phys. Chem. B* **2006**, *110*, 21014 – 21020.
[59] Y. Lu, C. Partridge, M. Meyyappan, J. Li, *J. Electroanal. Chem.* **2006**, *593*, 105 – 110.
[60] M. Penza, G. Cassano, R. Rossi, M. Alvisi, A. Rizzo, M. A. Signore, T. Dikonimos, E. Serra, R. Giorgi, *Appl. Phys. Lett.* **2007**, *90*, 173123.
[61] Y. X. Liang, Y. J. Chen, T. H. Wang, *Appl. Phys. Lett.* **2004**, *85*, 666 – 668.
[62] C. Bittencourt, A. Felten, E. H. Espinosa, R. Ionescu, E. Llobet, X. Correig, J. J. Pireaux, *Sens. Actuators B* **2006**, *115*, 33 – 41.
[63] N. D. Hoa, N. V. Quy, Y. S. Cho, D. Kim, *Phys. Status Solidi A* **2007**, *204*, 1820 – 1824.
[64] E. Bekyarova, M. Davis, T. Burch, M. E. Itkis, B. Zhao, S. Sunshine, R. C. Haddon, *J. Phys. Chem. B* **2004**, *108*, 19717 – 19720.
[65] T. Zhang, S. Mubeen, E. Bekyarova, B. Y. Yoo, R. C. Haddon, N. V. Myung, M. A. Deshusses, *Nanotechnology* **2007**, *18*, 165504.
[66] Y. Li, H. C. Wang, M. J. Yang, *Sens. Actuators B* **2007**, *121*, 496 – 500.
[67] P. Qi, O. Vermesh, M. Grecu, A. Javey, Q. Wang, H. Dai, S. Peng, K. J. Chao, *Nano Lett.* **2003**, *3*, 347 – 351.
[68] T. Zhang, M. B. Nix, B. Y. Yoo, M. A. Deshusses, N. V. Myung, *Electroanalysis* **2006**, *18*, 1153 – 1158.
[69] F. J. Owens, *Mater. Lett.* **2007**, *61*, 1997 – 1999.
[70] R. Czerw, M. Terrones, J. C. Charlier, X. Blase, B. Foley, R. Kamalakaran, N. Grobert, H. Terrones, D. Tekleab, P. M. Ajayan, W. Blau, M. Rühle, D. L. Carroll, *Nano Lett.* **2001**, *1*, 457 – 460.
[71] F. Villalpando-Páez, A. H. Romero, E. Munoz-Sandoval, L. M. Martínez, H. Terrones, M. Terrones, *Chem. Phys. Lett.* **2004**, *386*, 137 – 143.
[72] K. I. Lundström, M. S. Shivaraman, C. M. Svensson, *J. Appl. Phys.* **1975**, *46*, 3876 – 3881.
[73] J. Kong, M. G. Chapline, H. Dai, *Adv. Mater.* **2001**, *13*, 1384 – 1386.

[74] Y. M. Wong, W. P. Kang, J. L. Davidson, A. Wisitsora-at, K. L. Soh, *Sens. Actuators B* **2003**, *93*, 327 – 332.
[75] a) I. Sayago, E. Terrado, E. Lafuente, M. C. Horrillo, W. K. Maser, A. M. Benito, R. Navarro, E. P. Urriolabeitia, M. T. Martinez, J. Gutierrez, *Synth. Met.* **2005**, *148*, 15 – 19; b) I. Sayago, E. Terrado, M. Aleixandre, M. C. Horrillo, M. J. Fernández, J. Lozano, E. Lafuente, W. K. Maser, A. M. Benito, M. T. Martinez, J. Gutiérrez, E. Munoz, *Sens. Actuators B* **2007**, *122*, 75 – 80.
[76] J. Sippel-Oakley, H. T. Wang, B. S. Kang, Z. Wu, F. Ren, A. G. Rinzler, S. J. Pearton, *Nanotechnology* **2005**, *16*, 2218 – 2221.
[77] S. Dag, Y. Ozturk, S. Ciraci, T. Yildirim, *Phys. Rev. B* **2005**, *72*, 155404.
[78] M. K. Kumar, S. Ramaprabhu, *J. Phys. Chem. B* **2006**, *110*, 11291 – 11298.
[79] S. Mubeen, T. Zhang, B. Yoo, M. A. Deshusses, N. V. Myung, *J. Phys. Chem. C* **2007**, *111*, 6321 – 6327.
[80] a) Y. Sun, H. H. Wang, *Appl. Phys. Lett.* **2007**, *90*, 213107; b) Y. Sun, H. H. Wang, *Adv. Mater.* **2007**, *19*, 2818 – 2823.
[81] D. Ding, Z. Chen, S. Rajaputra, V. Singh, *Sens. Actuators B* **2007**, *124*, 12 – 17.
[82] A. Cusano, M. Consales, A. Cutolo, M. Penza, P. Aversa, M. Giordano, A. Guemes, *Appl. Phys. Lett.* **2006**, *89*, 201106.
[83] a) Y. Lu, J. Li, J. Han, H. T. Ng, C. Binder, C. Partridge, M. Meyyappan, *Chem. Phys. Lett.* **2004**, *391*, 344 – 348; b) J. Li, Y. Lu, H. T. Ng, J. Han, M. Meyyappan, *Chem. Senses* **2004**, *20(Suppl.B)*, 710 – 711.
[84] C. Matranga, B. Bockrath, *J. Phys. Chem. B* **2005**, *109*, 4853 – 4864.
[85] L. B. da Silva, S. B. Fagan, R. Mota, *Nano Lett.* **2004**, *4*, 65 – 67.
[86] S. Peng, K. Cho, *Nano Lett.* **2003**, *3*, 513 – 517.
[87] R. Wang, D. Zhang, W. Sun, Z. Han, C. Liu, *J. Molec. Struct.* **2007**, *806*, 93 – 97.
[88] O. K. Varghese, P. D. Kichambare, D. Gong, K. G. Ong, E. C. Dickey, C. A. Grimes, *Sens. Actuators B* **2001**, *81*, 32 – 41.
[89] a) S. Chopra, K. McGuire, N. Gothard, A. M. Rao, A. Pham, *Appl. Phys. Lett.* **2003**, *83*, 2280 – 2282; b) A. Zribi, A. Knoblock, R. Rao, *Appl. Phys. Lett.* **2005**, *86*, 203112.
[90] F. Picaud, R. Langlet, M. Arab, M. Devel, C. Giradet, S. Natarajan, S. Chopra, A. M. Rao, *J. Appl. Phys.* **2005**, *97*, 114316.
[91] Y. Wanna, N. Srisukhumbowornchai, A. Tauntranont, A. Wisitsoraat, N. Thavarungkul, P. Singjai, *J. Nanosci. Nanotechnol.* **2006**, *6*, 3893 – 3896.
[92] R. Q. Long, R. T. Yang, *Ind. Eng. Chem. Res.* **2001**, *40*, 4288 – 4291.
[93] J. Suehiro, G. Zhou, M. Hara, *Sens. Actuators B* **2005**, *105*, 164 – 169.
[94] P. G. Collins, K. Bradley, M. Ishigami, A. Zettl, *Science* **2000**, *287*, 1801 – 1804.
[95] K. Bradley, S. H. Jhi, P. G. Collins, J. Hone, M. L. Cohen, S. G. Louie, A. Zettl, *Phys. Rev. Lett.* **2000**, *85*, 4361 – 4364.
[96] V. Derycke, R. Martel, J. Appenzeller, P. Avoris, *Appl. Phys. Lett.* **2002**, *80*, 2773 – 2775.
[97] G. U. Sumanasekera, C. K. W. Adu, S. Fang, P. C. Eklund, *Phys. Rev. Lett.* **2000**, *85*, 1096 – 1099.
[98] D. C. Sorescu, K. D. Jordan, P. Avouris, *J. Phys. Chem. B* **2001**, *105*, 11227 – 11232.
[99] H. F. Kuo, D. H. Lien, W. K. Hsu, N. H. Tai, S. C. Chang, *J. Mater. Chem.* **2007**, *17*, 3581 – 3584.
[100] D. R. Kauffman, A. Star, *Nano Lett.* **2007**, *7*, 1863 – 1868.
[101] a) A. Zahab, L. Spina, P. Poncharal, C. Marlière, *Phys. Rev. B* **2000**, *62*, 10000 – 10003; b) P. S. Na, H. Kim, H. M. So, K. J. Kong, H. Chang, B. H. Ryu, Y. Choi, J. O. Lee, B. K. Kim, J. J. Kim, J. Kim, *Appl. Phys. Lett.* **2005**, *87*, 093101.
[102] P. C. P. Watts, N. Mureau, Z. Tang, Y. Miyajima, J. D. Carey, S. R. P. Silva, *Nanotechnology* **2007**, *18*, 175701.
[103] W. Kim, A. Javey, O. Vermesh, Q. Wang, Y. Li, H. Dai, *Nano Lett.* **2003**, *3*, 193 – 198.
[104] W. F. Jiang, S. H. Xiao, C. Y. Feng, H. Y. Li, X. J. Li, *Sens. Actuators B* **2007**, *125*, 651 – 655.
[105] X. Huang, Y. Sun, L. Wang, F. Meng, J. Liu, *Nanotechnology* **2004**, *15*, 1284 – 1288.
[106] a) K. Bradley, J. Cumings, A. Star, J. C. P. Gabriel, G. Grüner, *Nano Lett.* **2003**, *3*, 639 – 641; b) A. Star, T. R. Han, V. Joshi, J. R. Stetter, *Electroanalysis* **2004**, *16*, 108 – 112; c) H. W. Chen, R. J. Wu, K. H. Chan, Y. L. Sun, P.-G. Su, *Sens. Actuators B* **2005**, *104*, 80 – 84; d) P. G. Su, S. C. Huang, *Sens. Actuators B* **2006**, *113*, 142 – 149; e) H. Yu, T. Cao, L. Zhou, E. Gu, D. Yu, D. Jiang, *Sens. Actuators B* **2006**, *119*, 512 – 515; f) P. G. Su, C. S. Wang, *Sens. Actuators B* **2007**, *124*, 303 – 308.
[107] Z. M. Qi, M. Wei, I. Honma, H. Zhou, *ChemPhysChem* **2007**, *8*, 264 – 269.
[108] J. T. W. Yeow, J. P. M. She, *Nanotechnology* **2006**, *17*, 5441 – 5448.
[109] J. R. Huang, M. Q. Li, Z. Y. Huang, J. H. Liu, *Sens. Actuators A* **2006**, *133*, 467 – 471.
[110] a) Y. Zhang, K. Yu, R. Xu, D. Jiang, L. Luo, Z. Zhu, *Sens. Actuators A* **2005**, *120*, 142 – 146; b) P. G. Su, Y. L. Sun, C. C. Lin, *Sens. Actuators B* **2006**, *115*, 338 – 343.
[111] a) R. C. Fowler, *Rev. Sci. Instrum.* **1949**, *20*, 175 – 178; b) A. Berengo, A. Cutillo, *J. Appl. Physiol.* **1961**, *16*, 522 – 530.
[112] a) S. K. Pandey, K. H. Kim, *Sensors* **2007**, *7*, 1683 – 1696; b) M. R. Anderson, *J. Emerg. Nursing* **2006**, *32*, 149 – 153.
[113] K. G. Ong, C. A. Grimes, *Sensors* **2001**, *1*, 193 – 205.
[114] A. Star, T. R. Han, V. Joshi, J. C. P. Gabriel, G. Grüner, *Adv. Mater.* **2004**, *16*, 2049 – 2052.
[115] M. Gill, S. Walker, A. Khan, S. M. Green, L. Kim, S. Gray, B. Krauss, *Acad. Emerg. Med.* **2005**, *12*, 579 – 586.
[116] J. K. Robinson, M. J. Bollinger, J. W. Birks, *Anal. Chem.* **1999**, *71*, 5131 – 5136.
[117] O. Kuzmych, B. L. Allen, A. Star, *Nanotechnology* **2007**, *18*, 375502.
[118] a) D. A. Labianca, *J. Chem. Educ.* **1990**, *67*, 259 – 261; b) T. L. Brown, S. Gamon, P. Tester, R. Martin, K. Hosking, G. C. Bowkett, D. Gerostamoulos, M. L Grayson, *Antimicrob. Agents Chemother.* **2006**, *51*, 1107 – 1108.
[119] T. D. Ridder, S. P. Hendee, C. D. Brown, *Appl. Spectrosc.* **2005**, *59*, 181 – 189.
[120] C. M. Yang, H. Kanoh, K. Kaneko, M. Yudasaka, S. Iijima, *J. Phys. Chem. B* **2002**, *106*, 8994 – 8999.
[121] T. Someya, J. Small, P. Kim, C. Nuckolls, J. T. Yardley, *Nano Lett.* **2003**, *3*, 877 – 881.
[122] C. Cantalini, L. Valentini, I. Armentano, L. Lozzi, J. M. Kenny, S. Santucci, *Sens. Actuators B* **2003**, *95*, 195 – 202.
[123] a) M. Penza, F. Antolini, M. V. Antisari, *Sens. Actuators B* **2004**, *100*, 47 – 59; b) M. Penza, M. A. Tagliente, P. Aversa, M. Re, G. Cassano, *Nanotechnology* **2007**, *18*, 185502.
[124] C. Wei, L. Dai, A. Roy, T. B. Tolle, *J. Am. Chem. Soc.* **2006**, *128*, 1412 – 1413.
[125] a) M. Penza, G. Cassano, P. Aversa, F. Antolini, A. Cusano, A. Cutolo, M. Giordano, L. Nicolais, *Appl. Phys. Lett.* **2004**, *85*, 2379 – 2381; b) M. Penza, M. A. Tagliente, P. Aversa, G. Cassano, *Chem. Phys. Lett.* **2005**, *409*, 349 – 354; c) M. Penza, G. Cassano, P. Aversa, F. Antolini, A. Cusano, M. Consales, M. Giordano, L. Nicolais, *Sens. Actuators B* **2005**, *111–112*, 171 – 180; d) M. Penza, G. Cassano, P. Aversa, A. Cusano, A. Cutolo, M. Giordano, L. Nicolais, *Nanotechnology* **2005**, *16*, 2536 – 2547.
[126] a) A. Wisitsoraat, A. Tuantranont, C. Thanachayanont, V. Patthanasettakul, P. Singjai, *J. Electroceram.* **2006**, *17*, 45 – 49; b) Y. L. Liu, H. F. Yang, Y. Yang, Z. M. Liu, G. Li. Shen, R. Q. Yu, *Thin Solid Films* **2006**, *497*, 355 – 360.

[127] Y. Chen, C. Zhu, T. Wang, *Nanotechnology* **2006**, *17*, 3012 – 3017.
[128] L. Pauling, A. B. Robinson, R. Teranishi, P. Carey, *Proc. Natl. Acad. Sci. USA* **1971**, *68*, 2374 – 2376.
[129] S. M. Gordon, J. P. Szidon, B. K. Krotoszynski, R. D. Gibbons, H. J. O'Neill, *Clin. Chem.* **1985**, *31*, 1278 – 1282.
[130] a) M. Barker, M. Hengst, J. Schmid, H. J. Buers, B. Mittermaier, D. Klemp, R. Koppmann, *Eur. Respir. J.* **2006**, *27*, 929 – 936; b) C. L. Whittle, S. Fakharzadeh, J. Eades, G. Preti, *Ann. N. Y. Acad. Sci.* **2007**, *1098*, 252 – 266, and references therein.
[131] K. S. V. Santhanam, R. Sangoi, L. Fuller, *Sens. Actuators B* **2005**, *106*, 766 – 771.
[132] X. Ma, X. Zhang, Y. Li, G. Li, M. Wang, H. Chen, Y. Mi, *Macromol. Mater. Eng.* **2006**, *291*, 75 – 82.
[133] M. Sánchez, R. Guirado, M. E. Rincón, *J. Mater. Sci. Mater. Electron.* **2007**, *18*, 1131 – 1136.
[134] R. Wang, D. Zhang, Y. Zhang, C. Liu, *J. Phys. Chem. B* **2006**, *110*, 18267 – 18271.
[135] a) C. E. W. Hahn, *Analyst* **1998**, *123*, 57R – 86R; b) W. Cao, Y. Duan, *Crit. Rev. Anal. Chem.* **2007**, *37*, 3 – 13.
[136] For a discussion on the canine detection of explosives, see: a) K. G. Furton, L. J. Myers, *Talanta* **2001**, *54*, 487 – 500; for reviews on instrumentation for the detection of trace explosives, see: b) M. Nambayah, T. I. Quickenden, *Talanta* **2004**, *63*, 461 – 467; c) D. S. Moore, *Rev. Sci. Instrum.* **2004**, *75*, 2499 – 2512.
[137] For reviews on instrumentation for the detection of CWAs, see: a) Y. Seto, M. K. -Kataoka, K. Tsuge, I. Ohsawa, K. Matsushita, H. Sekiguchi, T. Itoi, K. Iura, Y. Sano, S. Yamashiro, *Sens. Actuators B* **2005**, *108*, 193 – 197; b) P. A. Smith, C. J. Lepage, K. L. Harrer, P. J. Brochu, *J. Occup. Environ. Hyg.* **2007**, *4*, 729 – 738.
[138] J. P. Novak, E. S. Snow, E. J. Houser, D. Park, J. L. Stepnowski, R. A. McGill, *Appl. Phys. Lett.* **2003**, *83*, 4026 – 4028.
[139] C. Y. Lee, M. S. Strano, *Langmuir* **2005**, *21*, 5192 – 5196.
[140] C. Y. Lee, S. Baik, J. Zhang, R. I. Masel, M. S. Strano, *J. Phys. Chem. B* **2006**, *110*, 11055 – 11061.
[141] K. Cattanach, R. D. Kulkarni, M. Kozlov, S. K. Manohar, *Nanotechnology* **2006**, *17*, 4123 – 4128.
[142] a) C. Staii, A. T. Johnson, M. Chen, A. Gelperin, *Nano Lett.* **2005**, *5*, 1774 – 1778; b) A. T. C. Johnson, C. Staii, M. Chen, S. Khamis, R. Johnson, M. L. Klein, A. Gelperin, *Phys. Status Solidi B* **2006**, *243*, 3252 – 3256.
[143] a) E. S. Snow, F. K. Perkins, E. J. Houser, S. C. Badescu, T. L. Reinecke, *Science* **2005**, *307*, 1942 – 1945; b) E. S. Snow, F. K. Perkins, J. A. Robinson, *Chem. Soc. Rev.* **2006**, *35*, 790 – 798.
[144] a) S. Kim, *Sensors* **2006**, *6*, 503 – 513; b) S. Kim, *Mod. Phys. Lett. B* **2005**, *19*, 1207 – 1211.
[145] a) B. Warneke, M. Last, b. Liebowitz, K. S. J. Pister, *Computer* **2001**, 44 – 51; b) M. J. Sailor, J. R. Link, *Chem. Commun.* **2005**, 1375 – 1383.
[146] E. Bekyarova, I. Kalinina, M. E. Itkis, L. Beer, N. Cabrera, R. C. Haddon, *J. Am. Chem. Soc.* **2007**, *129*, 10700 – 10706.
[147] D. Kauffman, A. Star, *J. Phys. Chem. C* **2008**, *112*, 4430-4434.
[148] F. Wang, H. Gu, T. M. Swager, *J. Am. Chem. Soc.* **2008**, *130*, 5392 – 5393.
[149] For a collection of papers detailing modern topics in chemical sensing, see: *Chem. Rev.* **2008**, *108*, 327 – 844.

